environments

Article

Modeling Flood-Prone Areas Using Statistical and GIS Approaches: Insights from the Yertis River Basin, Kazakhstan

Lyazzat Makhmudova [1], Sayat Alimkulov [1], Ainur Mussina [1,2,*], Elmira Talipova [1,2], Lyazzat Birimbayeva [1], Gaukhar Baspakova [1], Assel Abdullayeva [1,2], Bakyt Imamova [2], Alfiya Zagidullina [1], Zhomart Birimbayev [1,2,*], Tursyn Ibrayev [1], Marina Li [1] and Oirat Alzhanov [1,2]

[1] Institute of Geography and Water Security, Almaty 050000, Kazakhstan
[2] Department of Meteorology and Hydrology, Farabi University, Almaty 050040, Kazakhstan
* Correspondence: ainur.musina@kaznu.edu.kz (A.M.); bzm1987@mail.ru (Z.B.)

Abstract

Floods remain one of the most frequent and destructive natural phenomena, the scale and consequences of which are exacerbated by climate variability and anthropogenic pressure on river systems. The Yertis water basin (Kazakhstan) is an area with high exposure to flood risks, where the dense concentration of settlements and infrastructure is within floodplain areas. This study applies an integrated approach based on the integration of statistical methods for hydrological analysis and GIS-based spatial modeling to assess and delimit potential flood zones. Long-term series of maximum water levels and discharges from hydrological stations for the period 1974–2025 were analyzed using probability distribution functions, including the log-normal, Pearson Type III, and Gumbel distributions. The optimal distribution model for each station was selected based on the Kolmogorov–Smirnov goodness-of-fit test and the Akaike information criterion. Exceedance-probability curves for extreme hydrological events were constructed for 0.1%, 1%, and 10% probabilities. Spatial flood modeling was performed in the ArcGIS 10.8 environment using a hydrologically corrected digital elevation model and interpolated flood levels. The resulting flood zone maps allow for the identification of the highest-risk areas and serve as a tool for scientifically based planning of emergency prevention measures and floodplain area management. The study contributes to the methodological development of probabilistic floodplain mapping through the integration of statistical frequency analysis and GIS technologies and demonstrates the applicability of this approach for flood hazard assessment in large transboundary river systems under conditions of climatic and hydrological variability.

Keywords: Kazakhstan; Yertis River; hydrological hazards; floods; maximum water level; maximum water discharge; flood risk; flood-zone modeling

Check for updates

Academic Editor: Guobin Fu

Received: 27 April 2026
Revised: 25 May 2026
Accepted: 26 May 2026
Published: 28 May 2026

Copyright: © 2026 by the authors. Licensee MDPI, Basel, Switzerland. This article is an open access article distributed under the terms and conditions of the Creative Commons Attribution (CC BY) license.

1. Introduction

The safety of the population, social and economic facilities and the environment is one of the main conditions for the sustainable development of civilization. Protection against the negative impacts of natural hazards is a core component of national security programs. Even the economies of highly developed nations are unable to indefinitely increase funding for disaster relief and the recovery of associated losses. Consequently, it has become necessary to shift the focus of state policy toward disaster prevention aimed at risk reduction and mitigation, as prevention and mitigation of a threat are more effective than rescue in emerging emergency situations [1,2].

Since sustainability and security are the key challenges of the 21st century, a global effort is underway to develop not only a scientific framework for disaster risk management but also a specific system of programmatic measures to reduce risks and mitigate the consequences of emergencies [3].

The World Conference on Disaster Reduction, held from 18 to 22 January 2005, adopted the Framework for Action 2005–2015 (Hyogo Framework) following a review of the Yokohama Strategy. Overall, the Hyogo Framework for Action has provided critical guidance for disaster risk reduction efforts and contributed to the achievement of the Millennium Development Goals. The Hyogo Framework was developed to provide further momentum to the global action process mandated by the 1989 International Framework for Action for the International Decade for Natural Disaster Reduction, the 1994 Yokohama Strategy for a Safer World: Guidelines for Natural Disaster Prevention, Preparedness and Mitigation and its Plan of Action, and the 1999 International Strategy for Disaster Reduction [4].

Floods caused by spring freshets occur during heavy snowmelt. The intensity of a freshet is largely determined by the nature of the snowpack melting, as well as the depth of soil frost. The most hazardous situation is the rapid melting of a deep snowpack after winter, accompanied by heavy rainfall. In this case, all meltwater and rainwater run off over frozen ground directly into the river, which may result in a catastrophic freshet. Given the vastness of river floodplains and their active multi-purpose use, as well as the rapidity of spring freshet peaks, objective difficulties arise in adequately assessing damage during the inundation of territories. Floods caused by spring or spring–summer freshets are observed on rivers in almost all regions of Kazakhstan. The occurrence of this type of flood is likely on the rivers of Southern Kazakhstan in February–June, Southeastern and Eastern Kazakhstan—in March–July, and on the lowland rivers of the Republic–in March—June. The greatest damage is caused by floods on the Syrdariya, Yertis, Zhaiyk, Tobyl, Yesil, Zhabay, Nura, Torgay, Sarysu, and other rivers, as well as numerous tributaries. In most of the reviewed studies [5–10], flood hazard is investigated as a function of hydrological factors that lead to the disruption of economic activities. In the process of developing floodplain areas, inundation and waterlogging are automatically classified as floods of varying degrees of hazard, frequency, etc. [11,12]. In the present scientific study, the authors define floods as all extreme rises in the maximum water level involving the spillover of river waters onto the floodplain, which are or may be accompanied by damage to the population and its economic activities. When assessing flood hazards and risks, the morphometric characteristics of river basins and channel systems, including gradients, catchment area, basin shape, channel parameters, and topographic features, are of particular importance, as these factors largely determine the conditions under which flood processes form, spread, and intensify [13]. Additionally, the morphological and morphodynamic features of the territory that influence the development of hazardous hydrological phenomena are taken into account. The probability of potentially hazardous natural processes occurring within a specific time period is assessed through risk analysis, which allows for the determination of potential socioeconomic damage and the degree of threat to the population.

According to the report of the Intergovernmental Panel on Climate Change [14,15], floods are one of the most frequent natural disasters that cover large areas and surpass all other emergencies in terms of damage. In Kazakhstan, floods occupy a significant place among the dangerous natural phenomena that cause significant damage. There are about 800 rivers in the Republic (over 50 km long), more than 570 reservoirs of various capacities and various purposes, and about three thousand large lakes, the presence of which can be associated with floods. In recent decades, floods on the rivers of Kazakhstan have become more frequent, which is primarily due to anthropogenic reasons: unsatisfactory

flow regulation, development of flood-prone areas, conflicts of interest of water users, including at the interstate level.

According to studies [16], the significance of flood risk in Kazakhstan is further evidenced by estimates of average annual human losses. More than 390 fatalities occur per year, which is two-thirds higher than in any other CAREC (Central Asia Regional Economic Cooperation Program) member state, while it is expected that, on average, more than 156,000 people are affected by floods every year. The risk of floods in Kazakhstan is much more pronounced than the risk of earthquakes, as heavy rains and snowmelt cause significant damage. Average annual losses from flooding are estimated at 419 million USD. The spatial pattern of flood risk is diverse, with damages exceeding 30 million USD in many regions of Northern, Southern, and Central Kazakhstan. For a 100-year return period, flood losses are modeled at 1.8 billion USD, which represents approximately 1% of the Gross Domestic Product.

The modeling of flood-prone areas using statistical and GIS approaches is a rapidly evolving field of research [17,18]. Existing studies demonstrate the widespread application of various methodological approaches for assessing and mapping flood zones. In the field of statistical flood modeling, researchers have successfully applied frequency analysis of extreme discharge events. According to previous studies, the Shannon entropy model has been successfully applied to predict flood-prone areas, achieving an accuracy of 73.5% [19]. Logistic regression combined with GIS technologies has also demonstrated high efficiency in flood susceptibility mapping, with prediction accuracy reaching 85% [20]. GIS technologies are widely integrated with hydrological modeling approaches. Previous studies demonstrated the effectiveness of combining moisture indices with HEC-RAS hydraulic modeling [21]. In addition, multi-criteria GIS analysis based on the analytic hierarchy process has been used for flood hazard assessment, achieving a prediction accuracy of 74.90% (AUC-ROC) [22]. Recent studies have highlighted the effectiveness of probabilistic approaches for assessing urban flood risks associated with levee overtopping and multi-sectoral economic losses [23]. Comprehensive GIS-based MCDM frameworks have also been proposed for flood risk assessment under non-stationary hydrological conditions [24,25]. Advanced GIS-based approaches for flood hazard mapping in semi-arid urban regions have demonstrated the growing applicability of spatial modeling techniques in flood risk assessment [26]. Furthermore, probabilistic GIS-based frameworks integrating spatial analysis and probabilistic modeling techniques have been increasingly applied for urban flood risk assessment [27].

In Kazakhstan, several regional studies on flood hazard assessment have been conducted. One study developed a methodology for the Bukhtyrma River basin using 24 years of discharge observations and two-dimensional modeling, achieving an 87% agreement with satellite data [28]. Other studies developed GIS-based flood models for the Yesil River using remote sensing data [29]. Multi-criteria GIS analysis has also been applied to identify flood-prone areas in the city of Oskemen and to forecast floods caused by spring snowmelt [30,31].

Despite significant advances in flood modeling methodologies and the availability of regional studies in various river basins of Kazakhstan, there are still no comprehensive studies specifically dedicated to the Yertis River basin. This gap is particularly important considering the hydrological significance and transboundary nature of this river system for the region. The purpose of the current research is to model the flood zones of the area under consideration in combination with data on the maximum water levels and discharges during the flood period, determined at hydrological stations. The object of the study is the territory of the Yertis water basin, subject to seasonal flooding.

The scientific novelty of this work lies in the development and validation of a comprehensive approach to modeling flood zones, based on a combination of statistical methods for hydrological time series analysis and GIS technologies for spatial analysis. For the first time for the territory under consideration, the integration of statistical assessment results of the probabilistic characteristics of extreme hydrological events with digital elevation models and spatial data has been implemented, which will allow for clarifying the boundaries of flood zones and differentiating risk levels. The proposed approach provides a more detailed and objective representation of the spatial–temporal structure of floods and can serve as a methodological basis for further research in the field of natural risk assessment.

2. Materials and Methods

2.1. Study Area

The Yertis is the largest river in the Republic of Kazakhstan and a left tributary of the Ob River. The river flows through the territories of three neighboring countries: the People's Republic of China (512 km), the Republic of Kazakhstan (1696 km), and the Russian Federation (2040 km). The headwaters of the Yertis River are located on the border of Mongolia and the PRC on the eastern slopes of the Mongolian Altai Range (Figure 1). From the territory of the PRC, under the name Kara Yertis, the river passes through the Zhaysan Basin in Kazakhstan and flows into the through-flow Lake Zhaysan. In its upper reaches, before flowing into Lake Zhaysan, the Yertis River receives the right-bank tributary Alkabek and the high-water Kalzhyr, which flows out of Lake Markakol. In 1960, the dam of the Bukhtyrma Hydroelectric Power Plant was built below the mouth of the Bukhtyrma River. As a result of the backwater formed, the Bukhtyrma Reservoir, the largest in Kazakhstan, absorbed Lake Zhaysan. A number of Yertis River tributaries—the Kurshim, Naryn, Bukhtyrma, and others—flow into the Bukhtyrma Reservoir. Near the city of Oskemen, the dam of the Ust-Kamenogorsk Hydroelectric Power Plant was built on the Yertis River in 1953, forming the Ust-Kamenogorsk Reservoir. Below this dam, the right-bank tributary Ulbi flows into the Yertis River. Further downstream, near the village of Shalba, the third Shulbinsk Reservoir was created in 1988, into which the right-bank tributary of the Yertis River, the Oba River, flows.

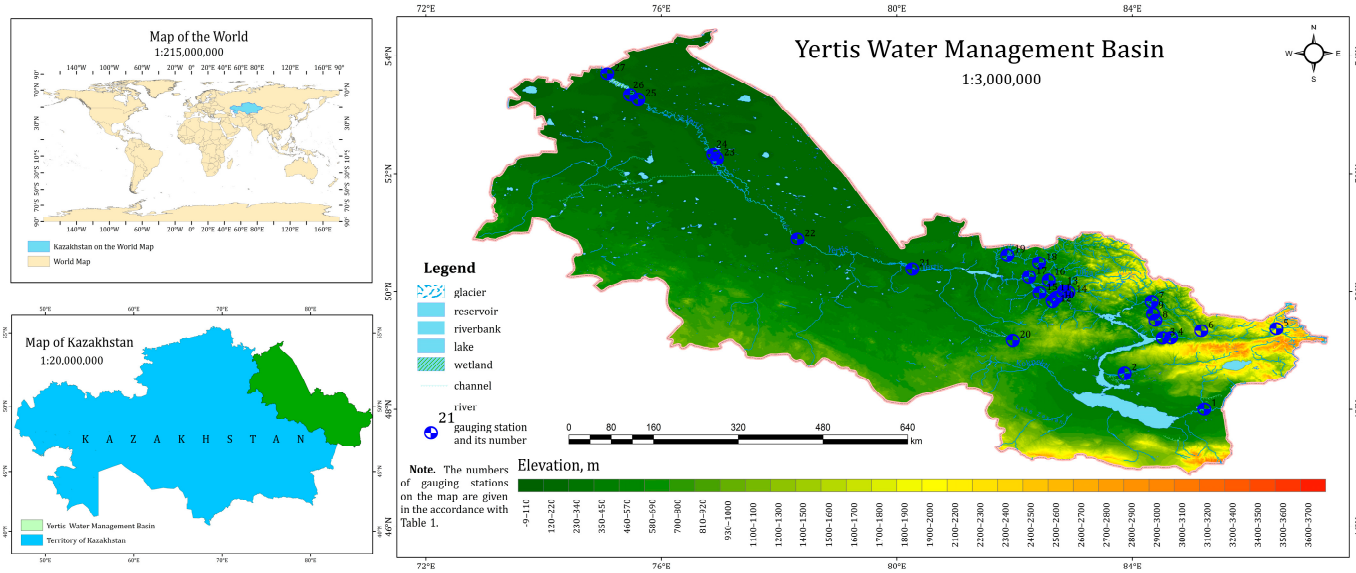

Figure 1. Overview map of the study area.

The Bukhtyrma, Oba, and Ulbi rivers are the largest and most high-water right-bank tributaries of the Yertis River. They form their runoff within the territory of the Kazakhstan

Altai, which possesses high moisture levels and a mountainous, highly dissected relief, which in turn determines the highest river network density and runoff depth in Eastern Kazakhstan. The rivers of the Southern Altai—the Karakoby, Akkoby, Alkabek, Kalzhyr, Kurshim, and Naryn—possess lower water availability.

The left-bank rivers—the Kendirlik, Uidene, Kandysu, Tebiske, Karboga, Bazar, Bugaz, Kokpekti, Ulken-Boken, Kyzylsu, Shar, and Shagan—are characterized by significantly lower water availability than the right-bank tributaries. During the low-flow period, some of these rivers lose their discharge in the lower reaches within loose channel deposits and do not reach the Yertis River.

It should be noted that 28 watercourses of the basin under consideration, including the Yertis River, are transboundary rivers. Most of the rivers of the considered water basin in mountainous areas are subject to floods and mudflows. The main factors of the spring flood of the rivers of the basin under consideration are the autumn moisture charge of soils, the maximum water reserves in the snow, the intensity of snowmelt and atmospheric precipitation during the formation of floods.

Table 1. List of hydrological stations in the Yertis River basin.

No.	The River is a Point	Catchment Area, km^2	Zero Mark of the Hydrological Station, m	Critical Marks of High-Water Levels Above the Zero Post, cm
1	Kara Yertis—Boran	55,900	404.16	525
2	Kurshim—Voznesenka	5840	474.18	310
3	Naryn—Ulken Naryn	1960	413.59	
4	Naryn—Kokbastau (Yubileynoye)	1541	420.5	479
5	Buktyrma—Berel	1850	1110.44	290
6	Buktyrma—Barlyk	6860	627.53	250
7	Buktyrma—Lesnaya Pristan	10,700	427.67	530
8	Left Berezovka—Sredigornoye	251	547.5	200
9	Berezovka—Solovyovo	755	325.6	293
10	Yertis—Abylaikit	147,000	284.88	300
11	Yertis—Ust-Kamenogorsk	146,000	328	
12	Abylaikit—Samsonovka	1600	280	350
13	Ulbi—Ulbi Perevalochnaya	4900	321.87	380
14	Kishi Ulbi—Gornaya Ulbinka	2170	348.42	380
15	Ulan—Gerasimovka	505	265	440
16	Glubochanka—Belokamenka	47	374.38	334
17	Krasnoyarka—Predgornoye	422	284	350
18	Oba—Verkhoba	4800	343.46	450
19	Oba—Shemonaikha	8470	289.02	430
20	Shar—Kentarlau	1800	500	490
21	Yertis—Semey	196,000	185.56	450
22	Yertis—Semiyarka	229,000	141.17	550
23	Yertis—Pavlodar	240,000	100.6	800
24	Yertis—Pavlodar (road bridge)	240,000	101.32	1084
25	Yertis—Zhanabet (Bobrovsky)	244,000	92.00	1282
26	Yertis—Yertis	245,000	85.62	1262
27	Yertis—Priirtyshskoye	250,438	78.81	1967

The Yertis River is among the largest rivers of interstate importance, with an average annual runoff of 33.8 m^3/year, of which 8.32 m^3/year enters as transit flow from the PRC, and 23.7 m^3/year is discharged beyond the Republic of Kazakhstan to the Russian Federation. The Yertis is of great economic significance—within Kazakhstan alone, more than 2 million people reside in the basin, which hosts major industrial centers such as Oskemen, Semey, and Pavlodar. The water supply for Central Kazakhstan is provided from the Yertis River, and the further development of energy, industry, and agriculture in these regions is directly linked to the utilization of the river's water resources.

2.2. Initial Data

This scientific study utilizes initial data from 25 hydrological posts (maximum levels, maximum discharges) for the period of 1974–2025, located on the official website of the Kazhydromet RSE [32]. The list of hydrological posts whose data were used for calculation and analysis is presented in Table 1; the locations of the hydrological posts within the Yertis River basin are demonstrated in Figure 1. Additionally, the calculation of inundation areas within settlements is based on archival records of the hydrological situation and data from hydrological posts in the territory under consideration.

2.3. Research Methods

2.3.1. Statistical Processing and Frequency Analysis of Hydrological Data

The methodological framework of this study combines hydrological–statistical analysis and GIS-based spatial modeling for probabilistic flood hazard assessment in the Yertis River basin. The overall flowchart of the study is presented in Figure 2.

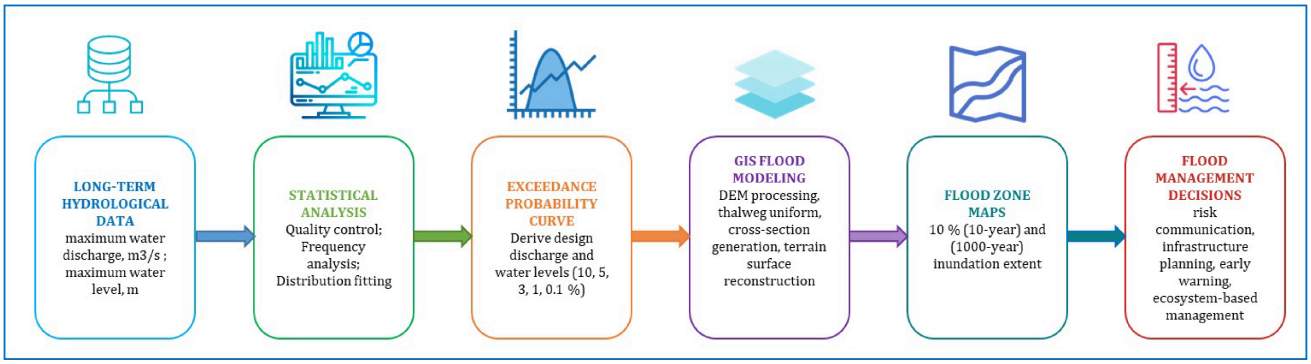

Figure 2. Flowchart of the methodological framework used in the study.

In many cases, a random variable (maximum, average annual, minimum water discharge, annual precipitation, etc.) can be used as a mathematical model to describe hydrometeorological phenomena. Each random variable is characterized by its own distribution probability. The analytical expression of the distribution probability is the distribution function (differential or integral) [33]. To provide a probabilistic description of hydrological extremes, the empirical data were approximated using theoretical distribution functions widely applied in hydrological frequency analysis, including the log-normal, Pearson Type III, and Gumbel distributions.1. Logarithmically normal distribution (many hydrological variables have a right-hand positive skewness, values usually exceed zero or some other lower limit, but are theoretically not limited by an upper limit, in such cases the distribution of a random variable does not correspond to the normal law) is an asymmetric distribution that can be reduced to a normal distribution by replacing the variable with its logarithm. The skewness coefficient of a logarithmically normal distribution is defined as follows [34]:

$$C_s = 3C_v + C_v^3 \quad (1)$$

where $C_v = \frac{\sigma}{m_x}$. For most hydrological variables $C_v < 1$, therefore, a good correspondence of empirical data with the log-normal distribution can be expected at $\frac{C_s}{C_v} = 3$–3.5.

In the practice of hydrological studies, the log-normal distribution is used in the calculation of the maximum flood flow. Along with the standard log-normal distribution, its various modifications are used (G.A. Alekseev's three-parameter log-normal distribution, for random variables with large asymmetry $C_s > 3.5C_v$).

1. The probability of distribution of extreme members of the sample (Gumbel distribution). This distribution probability was developed for the case when the extreme

characteristics of the hydrometeorological regime are considered as a random variable. The Gumbel security function is defined by the expression [35]:

$$P(x) = P\{X \geq x\} = 1 - exp[-exp(-y)] \quad (2)$$

The skewness coefficient for the Gumbel distribution is constant, and the graph P(x) of the function at high probability values goes into the negative range, significantly limiting the possibility of using the Gumbel distribution in the practice of hydrological research.

2. Pearson Distribution Type III (Continuous Binomial Distribution) [36]:

$$\frac{dy}{dz} = \frac{y(z+a)}{b_0 + b_1 z} \quad (3)$$

The Pearson Type III differential probability density curve starts from zero when $C_s = 2C_v$; it starts from a certain positive number when $C_s > 2C_v$, and extends into the region of negative values when $C_s < 2C_v$. The Pearson Type III exceedance-probability curve is, in the general case, a three-parameter curve and is defined by the parameters C_v, C_s, and a third parameter $m_x X$, which must be known to transition from modular coefficients to the values of the random variable X. Along with the conventional Pearson Type III curve, the log-Pearson Type III curve is used; this approach allows for shifting the curve out of the negative region when the ratio $C_s/C_v < 2$.

Empirical reliability was calculated by ranking the observations using the following formula [34,35]:

$$P = \frac{i}{n+1} \quad (4)$$

where i is the ordinal number of the value in the variation series, and n is the sample size.

The distribution for each hydrological station was not selected a priori, but rather on the basis of formal goodness-of-fit criteria [37–39].

The fit between the empirical and theoretical distributions was assessed using the Kolmogorov–Smirnov (K-S) test [40]:

$$D = max\left|F_{emp}(x) - F_{theor}(x)\right| \quad (5)$$

where $F_{emp}(x)$ is the empirical distribution function and $F_{theor}(x)$ is the theoretical distribution function. To provide a rough estimate of the approximation's validity, the following critical value was used [40,41]:

$$D_{crit} = \frac{1.36}{\sqrt{n}} \quad (6)$$

where n is the sample size.

The Akaike information criterion (AIC) was also used to compare the models [36]:

$$AIC = 2k - 2ln(L) \quad (7)$$

where k is the number of model parameters, and L is the maximum value of the likelihood function. The model with the minimum AIC value and an acceptable value of the D statistic was considered optimal.

The final selection of the distribution probability for each hydrological station was based on a combination of two criteria: the minimum AIC value and acceptable agreement between the empirical and theoretical distribution functions according to the Kolmogorov–Smirnov test. This approach significantly reduced the subjectivity of distribution selection and ensured the reproducibility of the statistical part of the study.

To verify the quality of the approximation of the empirical series by theoretical distribution probabilities, an additional validation of the selected models was performed [38,42]. A quantitative assessment of the quality of the reproduction of the empirical series was carried out using the following indicators [43]:

$$RMSE = \sqrt{\frac{1}{n}\sum_{i=1}^{n}(X_{obs,i} - X_{calc}, i)^2} \quad (8)$$

where $X_{obs,i}$ represents the observed values of maximum water discharge or water levels, X_{calc} represents the calculated values of maximum water discharge or water levels, and n represents the sample size.

Systematic Bias [43]:

$$Bias = \frac{1}{n}\sum_{i=1}^{n}(X_{\,calc}, i - X_{obs,i}) \quad (9)$$

Positive Bias values indicate that the model tends to overestimate the predicted values, while negative values indicate that it tends to underestimate them. The predicted values were determined based on the quantiles of the selected distribution for the empirical probabilities [44].

The evaluation of RMSE and Bias allows not only for the selection of a statistically acceptable model, but also for the quantitative characterization of the accuracy of reproducing the upper part of the distribution, which is most important for the analysis of extreme hydrological characteristics. R^2 was calculated between the empirical values and the corresponding calculated quantiles.

Undoubtedly, the supply curves are an important tool in the study and analysis of maximum water levels and discharges. Determining the probability of exceeding the maximum level is necessary for forecasting and planning measures to prevent and mitigate floods [45]. To approximate the distribution probabilities of specific hydrological quantities, the choice of the type of distribution function should be made taking into account the area of change in its argument.

The potential danger of floods for hydrological reasons, that is, without taking into account the social and economic factors, is determined by the degree of surprise and the height of flooding of the area by water. The rarer the flood, the greater its danger. The probability of flooding depends on the height of the floodplain and the highest water level. With a low floodplain, floods can occur almost annually. In this case, even at high historical water levels, the flood hazard is generally low as they are expected. A quantitative measure of the potential hazard of flooding due to hydrological causes is the value of D, which is determined by the following formula:

$$D = (H_{max,1\%} - H) \times (1 - p) \quad (10)$$

where $H_{max,1\%}$ is the maximum water level of 1% of the probability of exceedance; H—the mark of the beginning of floodplain flooding; p—the probability of floodplain flooding in fractions of one. Since there are a variety of methods for calculating the highest water levels, the highest water levels in the section of the hydrological station are determined by the analytical curve of the availability of their momentary or urgent values for the period of long-term observations.

2.3.2. Exceedance-Based Flood Inundation Modeling Using GIS

The assessment of potential flood inundation zones along the floodplain areas of the Yertis River was performed using a GIS-based geomorphological modeling approach

integrating a digital elevation model (DEM), river channel geometry, and probabilistic water-level scenarios (Figure 3).

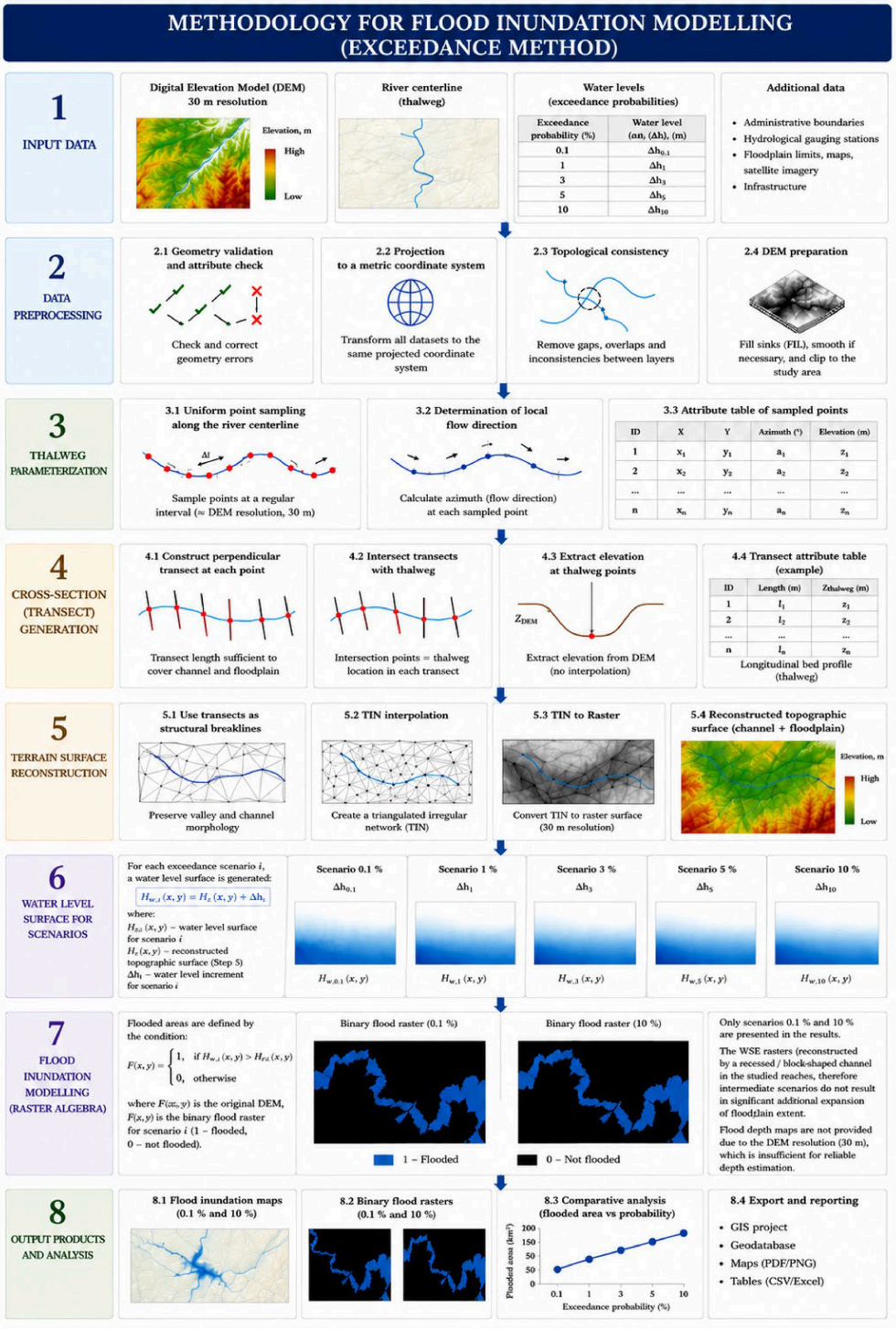

Figure 3. Methodology for flood inundation modeling (exceedance method).

Flood inundation modeling was conducted for the urban areas of Oskemen, Semey, and Pavlodar using exceedance probabilities of 0.1% and 10%. When applying this approach, the slopes of the water surface during flood events are assumed to be identical to the slopes derived from cartographic information of the main river channel [46,47].

The principal objective of this methodology is to represent the hydrological conditions of rivers relative to critical hydrological thresholds, including floodplain overflow levels, adverse hydrological events, and hazardous water levels recorded at hydrological stations.

To determine inundated areas, absolute water surface elevations were compared with terrain elevations extracted from the DEM. Areas where the simulated water level exceeded terrain elevation were classified as flooded zones. ArcGIS software was used for spatial analysis, terrain processing, interpolation procedures, and flood-zone delineation.

A DEM with a spatial resolution of 30 m was used as the primary topographic basis for terrain analysis and floodplain characterization, which is suitable for regional-scale assessments; however, higher-resolution terrain models are required for detailed urban flood simulations [48,49]. In this study, the DEM was used primarily for terrain representation, extraction of elevation marks, reconstruction of channel morphology, and identification of potentially flood-prone areas. Unlike fully hydrodynamic models, the applied approach does not simulate flow velocity or hydraulic interactions but instead relies on a geomorphologically conditioned comparison between reconstructed water surfaces and terrain elevations [50,51].

A linear vector layer representing the river centerline (thalweg) was used as the principal hydrographic framework defining the longitudinal structure of the river valley. All spatial datasets were transformed into a unified projected metric coordinate system and subjected to geometry validation and topological consistency checks. This preprocessing stage ensured spatial compatibility between raster and vector datasets and minimized systematic positional errors that could propagate during subsequent interpolation and inundation analysis.

To characterize longitudinal channel variability, the thalweg was parameterized by generating uniformly distributed reference points along the river axis. The spacing between points was selected according to the DEM resolution in order to preserve the spatial discreteness of the original elevation data and reduce longitudinal generalization effects.

For each reference point, the local channel direction was calculated automatically, after which transverse cross-sections perpendicular to the river centerline were generated. Automated transect construction ensured consistent orientation of cross-sections throughout the study area and eliminated subjective distortions associated with manual delineation [52]. The generated cross-sections extended across both the river channel and adjacent floodplain, allowing the representation of transverse valley morphology and potential floodwater propagation pathways.

Thalweg positions within each cross-section were determined through spatial intersection between the river axis and generated transects, ensuring strict topological consistency of the dataset. Elevation values at these locations were extracted directly from the DEM without additional interpolation in order to preserve original terrain characteristics and avoid artificial smoothing effects, which are critical for accurate representation of channel morphology.

Based on the extracted thalweg elevations and generated cross-sections, a continuous hydrologically consistent terrain surface was reconstructed using interpolation techniques (TIN and Topo to Raster) that incorporate structural breaklines. The cross-sections were used as geomorphological constraints preserving valley morphology, channel continuity, and floodplain structure during interpolation. This stage represents a key component of the modeling workflow because it enables realistic reconstruction of the river corridor prior to inundation simulation.

Flood inundation modeling was performed using raster algebra by comparing the reconstructed water-level surface with the DEM-derived terrain surface. For each exceedance-probability scenario (0.1% and 10%), an independent water-surface model was generated, enabling scenario-based assessment of floodplain expansion under different hydrological conditions. Modeling of flood zones was carried out on the basis of raster algebra by comparing the calculated surface of the water level with the original digital elevation

model. For each scenario of rare recurrence (0.1 and 10%), a separate water-level surface was formed according to the expression:

$$H_{w,i}(x,y) = H_t(x,y) + \Delta h_i \quad (11)$$

where $H_{w,i}(x,y)$ is the design surface of the water level for scenario i, $H_t(x,y)$ is the topographic surface of the channel and floodplain, and Δh_i is the excess of the water level corresponding to the specified availability.

Flood zones were determined on the basis of the logical condition of the water level exceeding the relief marks:

$$F_i(x,y) - \begin{cases} 1, & if\ H_{w,i}(x,y) > H_{dem}(x,y) \\ 0, & otherwise \end{cases} \quad (12)$$

where $H_{dem}(x,y)$ is the original digital elevation model, $F_i(x,y)$ is the binary flood-zone raster for Scenario i.

The resulting binary rasters represent the spatial distribution of inundated areas under different hydrological scenarios and enable analysis of flood-zone expansion dynamics depending on flood magnitude and exceedance probability. The final outputs included flood inundation maps, binary flood rasters, and comparative scenario-based assessments for the cities of Oskemen, Semey, and Pavlodar. In addition, a methodological workflow diagram illustrating the complete modeling sequence from DEM preprocessing and thalweg parameterization to terrain reconstruction and inundation mapping was incorporated into the manuscript to improve methodological transparency and reproducibility.

The applied approach is based on deterministic comparison of elevation surfaces and is widely used in regional flood assessments under conditions of limited hydrodynamic and hydraulic information [53–55].

The resulting inundation maps should therefore be interpreted as approximate spatial estimates of potential flood-prone areas derived from calculated maximum water levels and terrain morphology. Nevertheless, the methodology ensures reproducibility of results, formalization of calculations, and applicability for scenario-based flood-hazard assessment and spatial planning under data-limited conditions.

To quantitatively assess the uncertainty of the estimated extreme characteristics, a bootstrap approach was applied with repeated estimation of distribution parameters, taking into account both the variability of the original time series and the uncertainty of the parameters of the selected distributions [42,56]. For each hydrological station, an optimal distribution probability (log-normal distribution, Pearson Type III distribution, and Gumbel distribution) was determined at the preliminary stage based on the Kolmogorov–Smirnov criteria and the Akaike information criterion. Next, the bootstrap procedure was used to assess the stability of the calculated quantiles.

From the original time series of length n, N = 1000 bootstrap samples were formed using the with-replacement random sampling method. For each sample, the parameters of the previously selected distribution were re-estimated using the maximum likelihood method, after which the quantile corresponding to a 1% confidence level was calculated.

Thus, for each hydrological station, an empirical distribution of $Q_{1\%}$ quantile estimates were formed, based on which confidence intervals were determined:

$$Q_{low} = P_{2.5\%} \quad (13)$$

$$Q_{high} = P_{97.5\%} \quad (14)$$

where $P_{2.5\%}$ and $P_{97.5\%}$ are the 2.5th and 97.5th percentiles of the bootstrap distribution, respectively.

The width of the confidence interval was defined as:

$$\Delta = Q_{high} - Q_{low} \quad (15)$$

The relative uncertainty was estimated using the following formula:

$$U = \frac{Q_{high} - Q_{low}}{Q_{calc}} \times 100\% \quad (16)$$

where Q_{calc} is the calculated value of the 1% confidence quantile obtained from the original time series.

The use of a parametric bootstrap approach allows us to account for the sensitivity of the distribution tails to extreme values, as well as the impact of the limited length of the time series on the robustness of estimates of rare events.

3. Results

3.1. Maximum Water Levels

In the study area, the most hazardous hydrological processes affecting human activities are river flooding during spring high-water periods and the associated erosion processes, including riparian bank erosion and gully erosion. Additional hazards are associated with riverbank instability caused by fluctuations in water levels and flow dynamics [57]. Flooding is understood as spontaneous flooding of the land with water that has overflowed the banks as a result of melting snow, heavy downpours, surge or backwater phenomena. The danger of floods depends, first of all, on the height of the rise in the water level in the river [58]. The dynamics of maximum water levels in the Yertis River basin for the period 1974–2025 are considered to obtain an objective picture of the formation of extreme floods. The retrospective approach makes it possible to identify the most characteristic features of the hydrological regime and determine the years when extreme floods were observed (Figure 4).

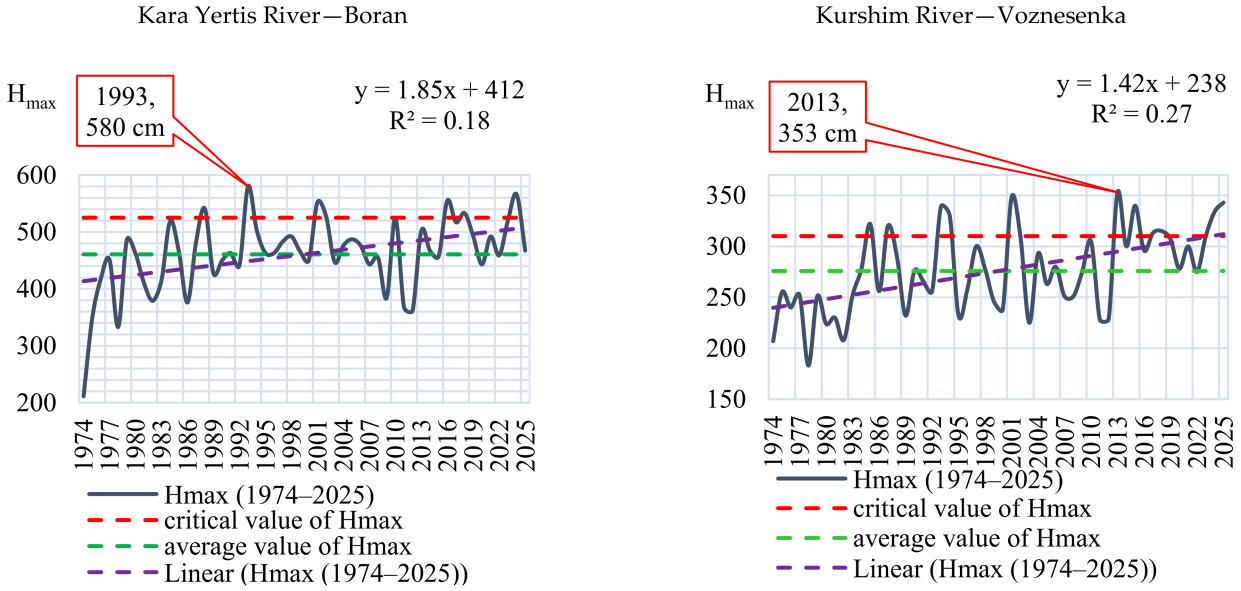

Figure 4. *Cont.*

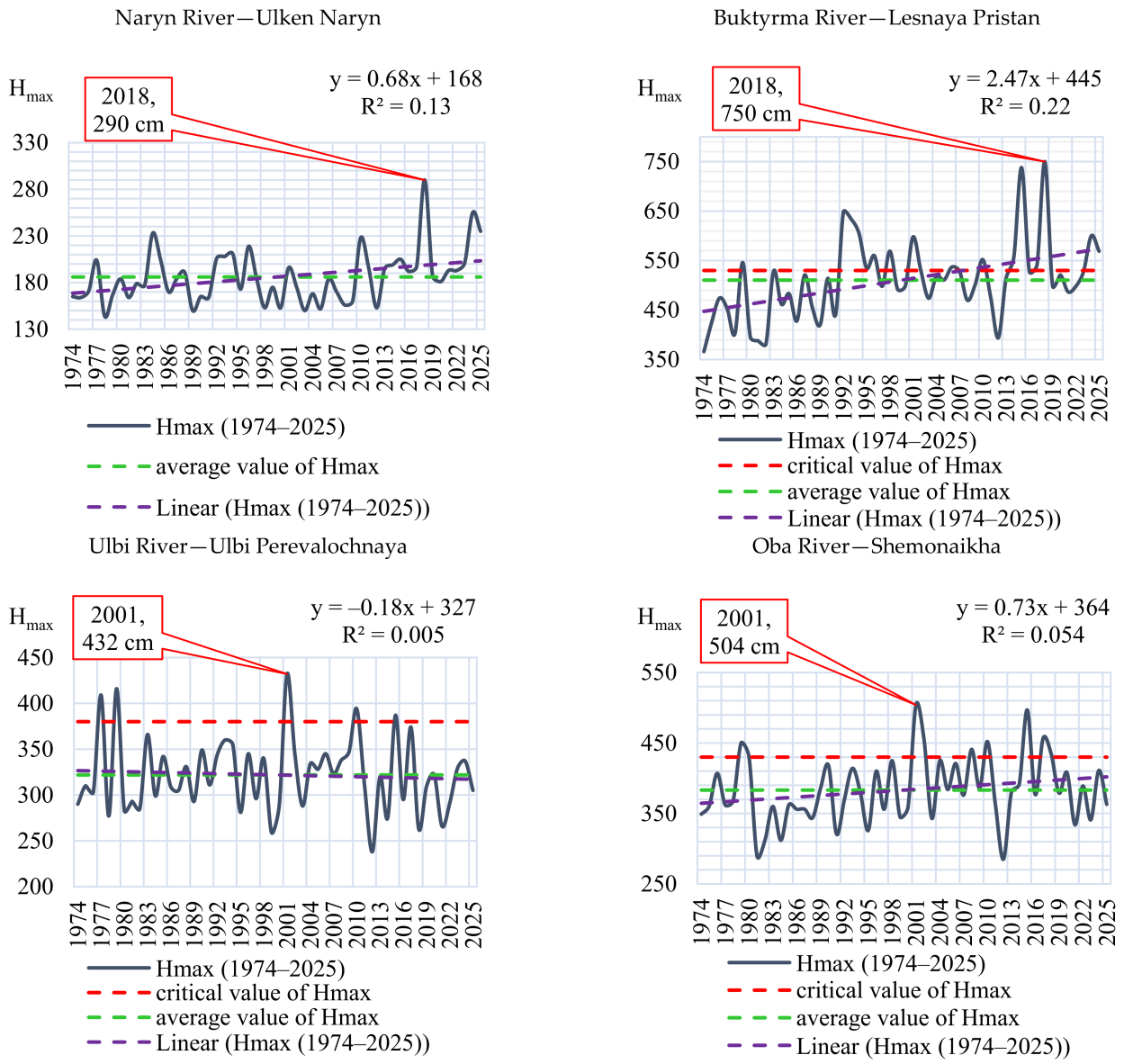

Figure 4. Dynamics of maximum water levels on the main rivers of the basin under consideration.

The next stage of the analysis was the construction of supply curves and the determination of the calculated parameters of the maximum water levels. The probabilistic approach provides a transition from the assessment and analysis of individual historical cases to a generalized assessment of the recurrence of extreme events in the river basin under consideration. An analysis of the time series of maximum water levels showed that the Pearson distribution is the best fit for some hydrological stations, while the log-normal distribution and the Gumbel distribution are the best fits for others (Table 2).

In most cases, the Kolmogorov–Smirnov statistics remained below the critical level, indicating acceptable agreement between the theoretical models and the empirical data series. An exception is the series from the Yertis—Pavlodar hydrological station, for which even the best of the models considered demonstrates comparatively weaker agreement with the empirical distribution, indicating the increased complexity of the statistical structure of this series and likely related to the influence of regulated flow and the transformation of the hydrological regime.

Table 2. Results of the distribution selection for the maximum water-level series.

River—Hydrological Station	Model	AIC	K-S Test, D	K-S Test, *p*-Value
Kara Yertis—Boran	Pearson Type III	581.41	0.108	0.542
Kurshim—Voznesenka	Log-normal	537.74	0.083	0.837
Naryn—Ulken Naryn	Gumbel	487.28	0.068	0.958
Buktyrma—Lesnaya Pristan	Log-normal	602.09	0.080	0.864
Yertis—Abylaikit	Pearson Type III	550.62	0.114	0.490
Ulbi—Ulbi Perevalochnaya	Log-normal	534.22	0.085	0.818
Oba—Shemonaikha	Log-normal	551.89	0.070	0.945
Yertis—Semey	Gumbel	540.47	0.061	0.984
Yertis—Semiyarka	Gumbel	590.97	0.109	0.539
Yertis—Pavlodar	Pearson Type III	562.41	0.194	0.037
Yertis—Zhanabet (Bobrovsky)	Pearson Type III	439.90	0.110	0.627
Yertis—Priirtyshskoye	Pearson Type III	549.78	0.059	0.988

To assess the quality of the approximation of the empirical series of maximum water levels, the RMSE, R^2, and Bias metrics were calculated for the selected distributions. The validation of the selected distributions for maximum water levels is presented in Table 3.

Table 3. Quality metrics for the approximation of selected distributions for maximum water-level series.

River—Hydrological Station	Model	RMSE	R^2	Bias
Kara Yertis—Boran	Pearson Type III	15.10	0.951	0.96
Kurshim—Voznesenka	Log-normal	5.29	0.987	−0.05
Naryn—Ulken Naryn	Gumbel	5.34	0.977	−0.85
Buktyrma—Lesnaya Pristan	Log-normal	14.66	0.966	0.39
Yertis—Abylaikit	Pearson Type III	11.95	0.959	−1.68
Ulbi—Ulbi Perevalochnaya	Log-normal	4.38	0.988	0.01
Oba—Shemonaikha	Log-normal	6.05	0.987	−0.38
Yertis—Semey	Gumbel	9.90	0.973	−1.06
Yertis—Semiyarka	Gumbel	18.15	0.970	−2.63
Yertis—Pavlodar	Pearson Type III	66.18	0.846	13.1
Yertis—Zhanabet (Bobrovsky)	Pearson Type III	8.27	0.964	1.31
Yertis—Priirtyshskoye	Pearson Type III	7.31	0.980	0.54

The poorest agreement was observed at the Yertis—Pavlodar hydrological station, which is attributed to the influence of regulating hydraulic structures; for most of the other hydrological stations, maximum water levels are reproduced with high accuracy—the RMSE does not exceed 18.15, and the Bias remains small in absolute terms.

Overall, the validation results confirm that the selected distribution probabilities are acceptable for the probabilistic assessment of extreme hydrological characteristics at the hydrological stations under consideration. However, for individual time series with a more complex regime, a more cautious interpretation of the obtained calculated parameters is required. Nevertheless, the validation performed showed good agreement between the calculated and empirical values. The resulting return period curves can be used for engineering calculations and the assessment of extreme hydrological characteristics at a given return period.

The constructed supply curves make it possible to obtain the values of maximum water levels of different probability of exceedance (0.1, 1, 3, 5, 10%), which are used both in the scientific substantiation of the regularities of the formation of high floods and in practical calculations for hydraulic engineering design and planning of flood control measures (Table 4).

Table 4. Maximum water levels corresponding to different exceedance probabilities for the period 1974–2025.

No.	River—Point	H_{avg}, cm	$H_{0.1\%}$, cm	$H_{1\%}$, cm	$H_{3\%}$, cm	$H_{5\%}$, cm	$H_{10\%}$, cm
1	Kara Yertis—Boran	460	689	625	590	572	545
2	Kurshim—Voznesenka	276	423	381	359	347	330
3	Naryn—Ulken Naryn	186	285	257	242	234	223
4	Buktyrma—Lesnaya Pristan	510	803	721	675	652	618
5	Yertis—Abylaikit	345	556	496	463	447	422
6	Ulbi—Ulbi Perevalochnaya	322	481	437	412	400	381
7	Oba—Shemonaikha	383	558	510	483	469	448
8	Yertis—Semey	440	641	586	555	539	515
9	Yertis—Semiyarka	418	724	636	589	564	528
10	Yertis—Pavlodar	677	841	811	794	785	770
11	Yertis—Zhanabet (Bobrovsky)	498	632	596	576	566	550
12	Yertis—Yertis	399	581	531	503	488	467
13	Yertis—Priirtyshskoye	677	834	792	769	756	738

Regarding the ratio of extreme water levels with a 0.1% exceedance probability ($H_{0.1\%}$) to the average water levels (H_{avg}), the analysis showed that the extreme levels exceed the average values by 1.23–1.73 times depending on the hydrological station (Figure 5). The highest ratio was observed at the Yertis—Semiyarka station, where $H_{0.1\%}$ exceeds the average level by 1.73 times (724 cm against 418 cm). High ratios were also identified at Yertis—Abylaikit (1.61 times) and Buktyrma—Lesnaya Pristan (1.57 times), indicating a significant increase in water levels during rare extreme flood events. In contrast, the lowest ratios were recorded at the downstream stations of the Yertis River, including Yertis—Priirtyshskoye (1.23 times) and Yertis—Pavlodar (1.24 times), which may reflect the regulating influence of reservoirs and a more stable river regime.

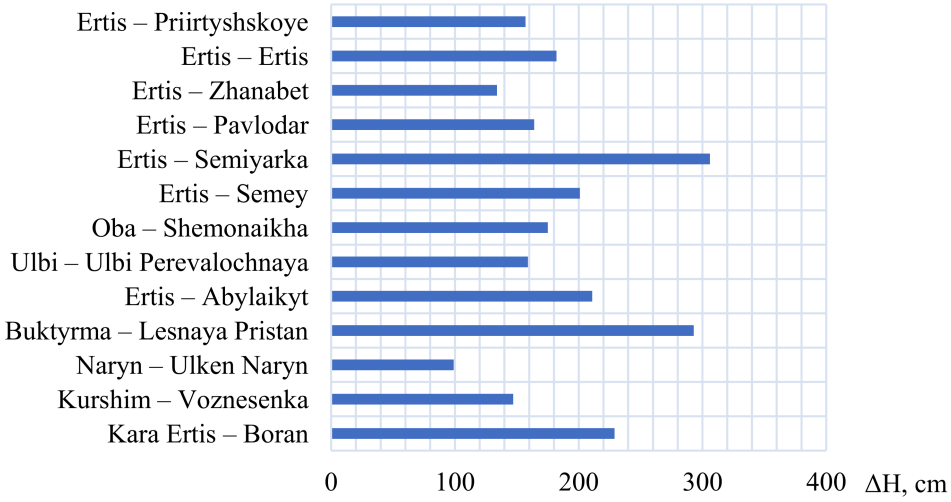

Figure 5. Range of excess of extreme levels $H_{0.1\%}$ above the mean values of H_{aver} of maximum water levels in the Yertis River basin.

The zone of increased risk of catastrophic floods is the middle course of the Yertis River (Semey—Pavlodar—Priirtyshskoye), at these hydrological stations, $H_{0.1\%}$ exceeds 800–1100 cm, which indicates the potential flooding of large areas in extreme years. This area is a priority in flood forecasting and the development of protective measures.

The observed frequencies of high-water levels leading to flooding in populated areas are presented in Table S1 on the recurrence and probability of maximum water levels in the Yertis River, and the key parameters of maximum water levels are presented in Table 5.

Table 5. Key characteristics of maximum water-level variability and flood recurrence at hydrological posts of the Yertis River basin.

The River is a Hydrological Post	Range of Maximum Water Level, cm	Frequency of Water Levels with ≤10% Exceedance Probability	Main Trends
Kara Yertis—Boran	210–580	1988, 1993, 2001, 2016, and 2024 (5 events).	Moderate variability with periodic high-water events in recent decades
Kurshim—Voznesenka	180–360	1993, 2001, 2013, 2015, 2024, and 2025 (6 events).	Predominance of medium and moderate floods
Naryn—Ulken Naryn	150–270	Extreme floods were recorded in 1984, 2010, 2018, 2024, and 2025 (5 events).	Relatively stable regime with moderate fluctuations
Buktyrma—Lesnaya Pristan	360–750	1992, 1993, 1994, 2015, and 2018 (5 events).	One of the highest amplitudes of water-level fluctuations
Yertis—Abylaikit	260–500	1976, 1985, 1987, 1988, and 2016 (5 events).	Gradual decrease in extremely high-water occurrences after the 1990s
Ulbi—Ulbi Perevalochnaya	230–440	1977, 1979, 2001, 2010, and 2015 (5 events).	Stable occurrence of moderate floods with episodic extremes
Oba—Shemonaikha	280–510	2001, 2002, 2010, 2015, and 2017 (5 events).	Frequent medium floods and a relatively stable hydrological regime
Yertis—Semey	340–640	1974, 1984, 1985, 1981, 1982, 2014, and 2018 (7 events).	Decrease in frequency of exceptionally high floods after 2000
Yertis—Semiyarka	270–710	1977, 1980, 1985, 1989, 1992, 2008, and 2014 (7 events).	Significant long-term variability and periodic extreme inundations
Yertis—Pavlodar	270–790	1988, 1990, 1994, 2010, 2013, 2015, 2017, 2018, 2020, 2024, and 2025 (11 events).	Regulated flow regime with relatively stable high-water levels
Yertis—Priirtyshskoye	520–780	1988, 2001, 2015, 2016, 2017, 2020, 2021, and 2024 (8 events).	High but regulated water levels with reduced variability downstream

An analysis of the recurrence of high-water levels with a probability of 10% or less revealed significant spatial heterogeneity in the occurrence of extreme hydrological events in the Yertis River basin. In general, the highest recurrence of extreme water levels is characteristic of the lower and middle reaches of the Yertis River, whereas the mountain tributaries are characterized by fewer rare high-water events.

The analysis showed that since 2010, an increase in the recurrence of extremely high-water levels has been observed at a number of gauging stations. This may indicate an intensification of the influence of climate variability, changes in snowmelt conditions, and an increase in the frequency of anomalous hydrometeorological processes in the Yertis River basin.

By superimposing the height of the maximum water levels on the absolute elevations of the hydrological stations, the elevations of the absolute heights of the flooded area during floods of 0.1%, 10% of the probability for each settlement of the study area were determined (Figure 6).

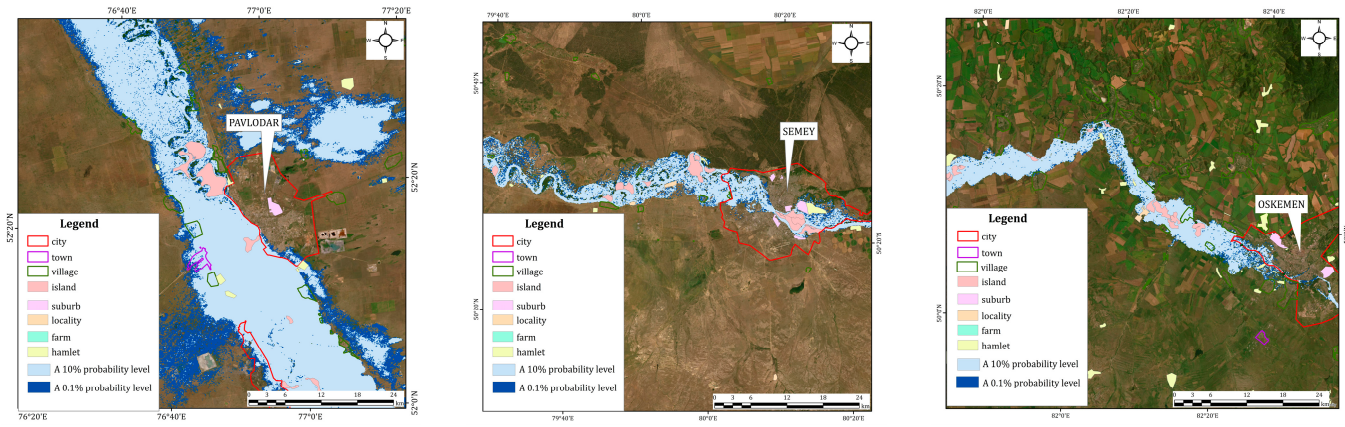

(**a**) Pavlodar city (**b**) Semey city (**c**) Oskemen city

Figure 6. Maps of flood zones (maximum water levels of 0.1 and 10% probability) of large cities in the basin under consideration.

Within the framework of this study, cross-sites located near three large urbanized and industrially developed centers—the cities of Pavlodar, Semey and Oskemen—were selected for modeling. The choice of these sites is due to their strategic importance, high population density, developed infrastructure, and historically recorded cases of flooding. The choice of the Pavlodar, Semey and Oskemen sites is due to the fact that these areas are exposed to high-water levels and ice phenomena. In the area of Oskemen, in some years, cases of floodplain areas, rising groundwater and flooding of dacha areas were recorded, which is associated with both the natural regime of the river and the regulation of flow by a cascade of hydroelectric power plants. In the city of Pavlodar, flood situations repeatedly led to flooding of floodplain areas and low-lying areas, which required flood control measures and temporary evacuation of the population.

Analysis of archival and official data indicates repeated flood impacts on the areas under consideration. In the Beskaragai district, five cases of flooding were recorded: in the village of Beskaragai (2017, 2019 and 2021), in the village of Krivinka and the village of Glukhovka (2015), as well as in the villages of Boztal and Karabas (2024). Within the boundaries of the city of Semey and adjacent settlements, flooding was observed in 2014 and 2018 (Semey city), in 2017 (near the village of Taldy) and in 2024 (Karakol village).

Especially indicative is the flood event of 29 March 2018, when, due to a sharp rise in the water level in the Yertis River in the city of Semey, 141 residential buildings and 596 summer houses were flooded, which required the evacuation of more than 220 people, this information is based on the official materials of the flood situation analysis provided by the Department of Emergency Situations of the Abai region for 2024.

Consequently, the selected sites are characterized by a high frequency of flood events, significant potential damage and the need for scientifically based forecasting and management of flood risks, which makes them representative and justified for hydrological modeling within the framework of this study.

An analysis of hydrological characteristics has shown that the 10% return period water levels in the areas under consideration consistently exceed the long-term average values (Table 4). Thus, in the Oskemen area, the excess averages 0.4–0.6 m; in the Semey area, it is approximately 0.7–0.8 m; and in the Pavlodar area, it reaches 0.9–1.0 m. The obtained values indicate that even relatively frequent floods (10% probability) lead to a significant increase in river water levels and water overflowing the riverbed.

An analysis of the recurrence of maximum water levels (Table 6) showed that levels corresponding to a 10% probability occur approximately every 8–12 years, which is confirmed by the frequency distribution in the long-term observation series (1974–2025). It was also found that in the upper reaches of the river, such levels occur less frequently and are characterized by greater interannual variability, whereas in the middle and lower reaches (the Semey and Pavlodar regions), their recurrence is higher, and the range of level fluctuations is more smoothed out. This indicates differences in the river's hydrological regime, caused by both natural (channel and floodplain morphology) and hydrological factors.

The results of spatial modeling showed that at 10% probability water levels, significant flood zones form, the nature of which varies substantially along the river's length. In the area of Oskemen, flooding is predominantly local in nature and is limited to low-lying sections of the floodplain. In the area of Semey, there is a sharp increase in the flood area and the formation of spatially connected inundation zones, indicating the territory's high sensitivity to flood impacts. In the lower reaches (Pavlodar), flooding is characterized by a significant extent and covers vast sections of the floodplain, which is due to the gentle slope of the terrain and the wide river valley.

Table 6. Results of statistical analysis of time series of maximum water discharges in the main rivers of the Yertis River basin.

No.	River—Hydrological Post	$\overline{Q}$, m³/s	Q_{max} (Year)	Q_{min} (Year)	σ, m³/s	M, m³/s
1	Kara Yertis—Boran	1314	2180 (1993)	451 (2012)	364	1310
2	Kurshim—Voznesenka	471	963 (1993)	166 (2011)	199	430
3	Naryn—Ulken Naryn	48.6	166 (2018)	18.7 (1982)	26.5	46.0
4	Buktyrma—Lesnaya Pristan	1370	2740 (2015)	629 (2012)	390	1300
5	Ulbi—Ulbi Perevalochnaya	910	2220 (1979)	441 (2011)	360	850
6	Both are Shemonaikha	1610	2900 (1979)	334 (2021)	500	1580
7	Shar—Kentarlau	49	119 (2013)	12.9 (1982)	24	47
8	Yertis—Semiyarka	3620	4420 (1994)	1900 (2012)	400	3610

Note: $\overline{Q}$ is an average value of the maximum water discharge for the period 1974–2025, Q_{max} is the maximum value of the maximum water discharge in the sample, Q_{min} is the lowest value of the maximum water discharge in the sample, σ—standard deviation, M—median.

Additionally, it was found that under a 10% probability flood scenario, a significant portion of the urban area falls within the flood zone. In percentage terms, the flooded area amounts to 6.1% for Oskemen, 13.6% for Semey, and 4.3% for Pavlodar. These results demonstrate a high level of potential exposure for urbanized areas and confirm the need to account for medium-probability scenarios in spatial planning and the development of flood mitigation measures. The analysis showed that 10% return period floods play a key role in the formation of inundation zones and are characterized by pronounced spatial heterogeneity. The highest vulnerability was identified in the middle and lower reaches of the Yertis River, where the combination of hydrological conditions and floodplain morphology contributes to the development of large-scale flooding even during relatively frequent flood events.

3.2. Maximum Water Discharge

The dynamics of maximum water discharges are considered to identify long-term trends in changes in extreme flow. Analysis of time series of maximum water discharges makes it possible to establish the regularities of their fluctuations, to determine the periods of high and low water content, and to assess the frequency and intensity of extreme floods. Figure 7 shows the dynamics of maximum water discharges on the main rivers of the basin under consideration.

An analysis of maximum discharge data (Figure 5) from hydrological stations in the Yertis River basin reveals significant interannual variability and cyclical patterns in the hydrological regime. The highest water flows are observed on large rivers and mountain tributaries (Buktyrma, Oba, Ulbi, Yertis-Semiyarka), where extreme floods occur on average once every 7–12 years. Small and medium-sized rivers (Naryn, Shar, Kurshim) are also characterized by high variability, although absolute discharge values are significantly lower.

In recent years, an increase in the recurrence of extremely high-water discharges and a widening of the range of flow fluctuations have been observed at the hydrological stations Kara Yertis—Boran, Buktyrma—Lesnaya Pristan, Oba—Shemonaikha, and Kurshim—Voznesenka, indicating increased climatic instability and more frequent dangerous flood events. The Naryn—Ulken Naryn and Shar—Kentarlau stations are also characterized by high interannual variability, linked to the dependence of flow on seasonal climatic factors. At the same time, at the Ulbi—Ulbi Perevalochna station, a decrease in the amplitude of fluctuations in maximum water discharge was observed during the 2015–2025 period, while at the Yertis—Semiyarka station, a relatively stable regime of high-water levels persists. Overall, the hydrological regime of the Yertis River basin is characterized by increased variability and a trend toward more frequent extreme spring floods. Table 6 presents the

results of statistical analysis of the time series of maximum water discharges of the main rivers of the Yertis River basin.

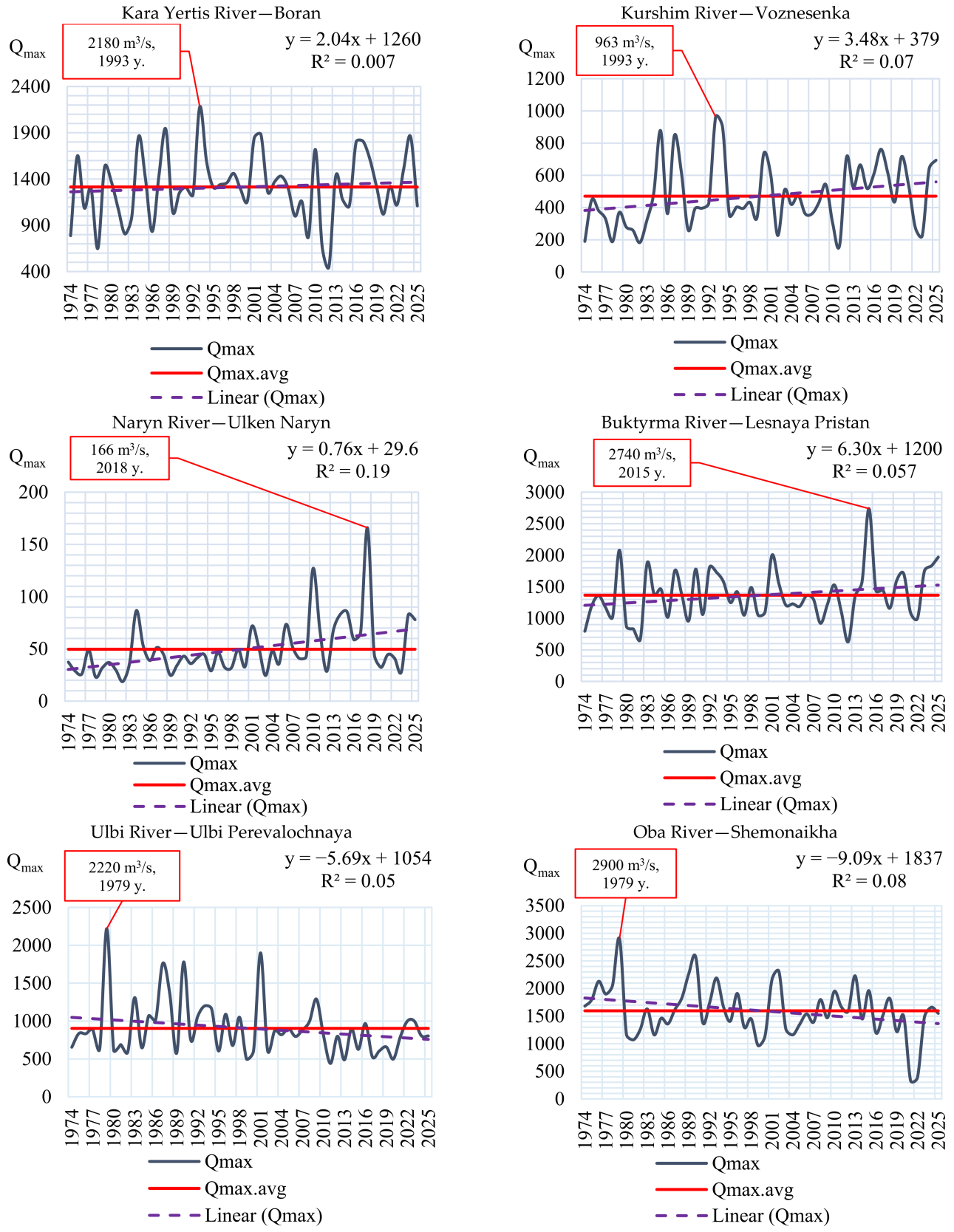

Figure 7. *Cont.*

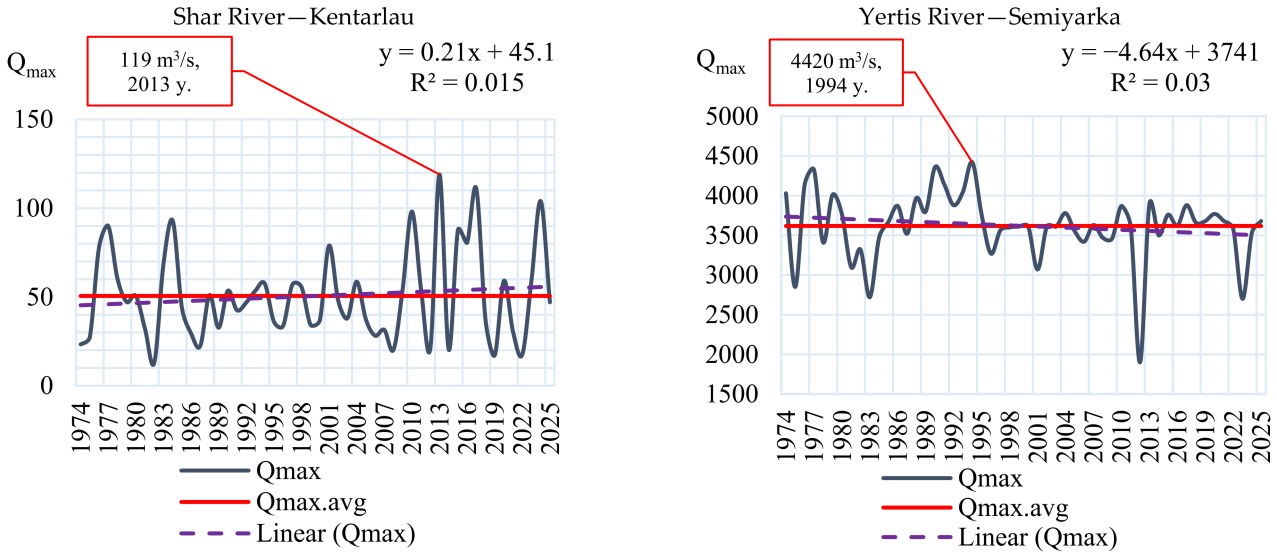

Figure 7. Dynamics of maximum water discharge on the main rivers of the basin under consideration.

The rivers of the basin under consideration have high absolute discharges, extremes exceeding the long-term average values of maximum water discharges by 1.5–2 times are recorded. Small rivers (Naryn, Shar) are characterized by low absolute values, but high relative variability, which makes them sensitive to climatic fluctuations. Extreme years (1979, 1993, 1994, 2013, 2015, 2018) are control years for assessing flood risks, since during these periods the maximum values were recorded on most watercourses of the basin under study. The standard deviation confirms that the Ulbi and Oba rivers are the most variable, and the Yertis is the least variable, which is related to the scale and storage capacity of the basin.

A comparison of the log-normal distribution, the Pearson III distribution, and the Gumbel distribution revealed that a single distribution function is not optimal for all hydrological stations. For the maximum discharge series at a number of hydrological stations, the Pearson III distribution showed the best agreement with empirical data, which is consistent with the asymmetric nature of the distribution of flood peaks. For other hydrological stations, the log-normal model proved to be the best fit, and in one case, the Gumbel distribution. Consequently, the choice of distribution function must be made individually for each hydrological station (Table 7).

Table 7. Results of the distribution selection for the maximum water flow series.

River—Hydrological Station	Model	AIC	K-S Test, D	K-S Test, *p*-Value
Kara Yertis—Boran	Pearson Type III	765.80	0.074	0.920
Kurshim—Voznesenka	Log-normal	695.71	0.070	0.946
Naryn—Ulken Naryn	Log-normal	460.63	0.098	0.668
Buktyrma—Lesnaya Pristan	Log-normal	769.90	0.059	0.988
Ulbi—Ulbi Perevalochnaya	Pearson Type III	743.04	0.085	0.811
Oba—Shemonaikha	Gumbel	802.53	0.132	0.297
Shar—Kentarlau	Log-normal	477.74	0.079	0.874
Yertis—Ust-Kamenogorsk	Pearson Type III	746.53	0.119	0.447
Yertis—Semiyarka	Pearson Type III	776.45	0.126	0.356

In general, the Pearson III distribution tended to yield the lowest AIC values, whereas the log-normal distribution performed better for time series exhibiting pronounced positive skewness.

To assess the quality of the approximation of the empirical maximum water discharge series, the RMSE, R^2, and Bias metrics were calculated for the selected distributions. The validation of the selected distributions for maximum water discharge is presented in Table 8.

Table 8. Quality metrics for the approximation of selected distributions for the maximum water discharge series.

River—Hydrological Station	Model	RMSE	R^2	Bias
Kara Yertis—Boran	Pearson Type III	48.64	0.985	−0.18
Kurshim—Voznesenka	Log-normal	23.42	0.989	−4.71
Naryn—Ulken Naryn	Log-normal	6.89	0.957	−1.14
Buktyrma—Lesnaya Pristan	Log-normal	57.92	0.979	−0.83
Ulbi—Ulbi Perevalochnaya	Pearson Type III	77.41	0.968	−10.5
Oba—Shemonaikha	Gumbel	99.02	0.957	−0.13
Shar—Kentarlau	Log-normal	3.04	0.988	−0.69
Yertis—Ust-Kamenogorsk	Pearson Type III	151.96	0.895	−15.9
Yertis—Semiyarka	Pearson Type III	130.62	0.910	5.54

The results showed that, overall, the models used demonstrate acceptable agreement with the empirical data series, as evidenced by high values of the coefficient of determination, which range from 0.895 to 0.989. The highest approximation quality was obtained for the following hydrological stations: Kara Yertis—Boran, Kurshim—Voznesenka, and Shar—Kentarlau, where R^2 exceeds 0.98, and RMSE remains relatively low. The most difficult series to approximate were Yertis—Ust-Kamenogorsk and Yertis—Semiyarka, for which the RMSE reaches 151.96 and 130.62, respectively, which is associated with a greater amplitude of interannual variability in maximum discharges. At the same time, the Bias values are close to zero in most cases, indicating the absence of a pronounced Systematic Bias in the model.

To assess the structure and recurrence of spring floods, the distribution of maximum water discharges by categories was carried out (Table 9). This approach makes it possible to identify characteristic runoff ranges, the frequency of their occurrence and the proportion of extreme values for the analysis of hydrological hazard and flood forecasting.

Table 9. Frequency distribution of maximum water discharges in the main rivers of the Yertis River basin.

Category	Frequency	Share, %	Graphic Interpretation
Kara Yertis River—Boran			
<800	5	10	
801–1200	14	27	
1201–1600	22	42	
1601–2000	10	19	
>2000	1	2	
Kurshim River—Voznesenka			
166–350	14	27	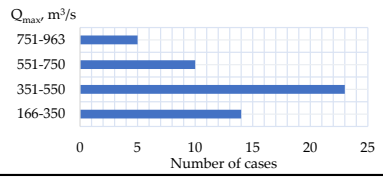
351–550	23	44	
551–750	10	19	
751–963	5	10	

Table 9. *Cont.*

Category	Frequency	Share, %	Graphic Interpretation
Naryn River—Ulken Naryn			
18–55	22	42	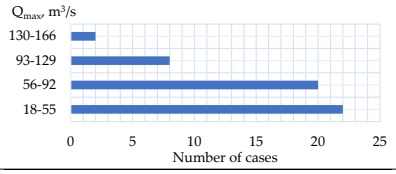
56–92	20	39	
93–129	8	15	
130–166	2	4	
Buktyrma River—Lesnaya Pristan			
<1000	6	11	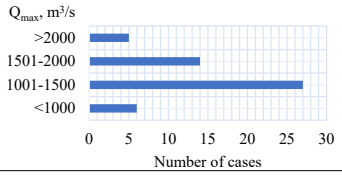
1001–1500	27	52	
1501–2000	14	27	
>2000	5	10	
Ulbi River—Ulbi Perevalochnaya			
<700	14	27	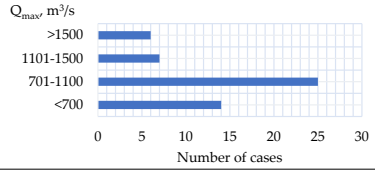
701–1100	25	48	
1101–1500	7	13	
>1500	6	12	
Oba River—Shemonaikha			
<1000	5	10	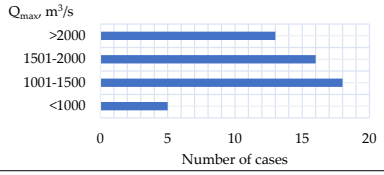
1001–1500	18	35	
1501–2000	16	31	
>2000	13	25	
Shar River—Kentarlau			
<30	10	19	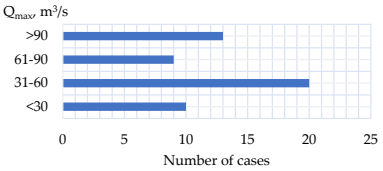
31–60	20	39	
61–90	9	17	
>90	13	25	
Yertis River—Semiyarka			
<3000	3	6	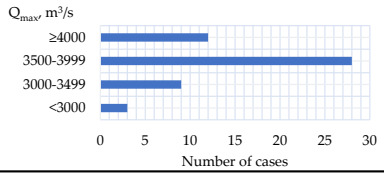
3000–3499	9	17	
3500–3999	28	54	
≥4000	12	23	

Small rivers (Kurshim, Naryn, Shar) are stable, but at the same time, even small absolute extremes can pose a local hazard. The tributaries of the Ulbi, Oba, and Buktyrma demonstrate high variability and a significant share of extreme discharges (>1500 m^3/s). The main artery of the Yertis River basin is characterized by high stability, but the extremes (>4000 m^3/s) are observed frequently (23%), which is a key factor in the flood danger of the region. In general, the distribution of maximum water discharges indicates an increase in the probability of extreme floods in the basin under consideration, which requires differentiated risk management and a revision of the provision of maximum water discharges.

Calculation of the exceedance probability of maximum water discharges: The calculation of exceedance probabilities for maximum water discharges directly characterizes the quantity of water passing through a river gauging station during the spring freshet period. Maximum water levels are important for assessing inundations and constructing vulnerability maps of territories. In turn, maximum water discharges reflect runoff intensity and serve as the basis for the calculated characteristic during:

- Design and operation of hydraulic structures.
- Assessment of water Determination of the capacity of channels and floodplains.
- Management and environmental risks associated with extreme floods.
- Hydrological substantiation of flood control measures and territory protection systems.
- Scenario forecast of the consequences of climate change.

Table 10 shows the maximum water discharges of different availability of the Yertis River basin under consideration.

Table 10. Maximum water discharges of different availability for the period 1974–2025.

No.	River—Point	$Q_{0.1\%}$, m^3/s	$Q_{1\%}$, m^3/s	$Q_{3\%}$, m^3/s	$Q_{5\%}$, m^3/s	$Q_{10\%}$, m^3/s
1	Kara Yertis—Boran	2695	2279	2061	1949	1785
2	Kurshim—Voznesenka	1323	1048	905	836	736
3	Naryn—Ulken Naryn	177	134	112	101	85.6
4	Buktyrma—Lesnaya Pristan	2928	2453	2205	2079	1894
5	Yertis—Ust-Kamenogorsk	3279	2651	2322	2162	1927
6	Ulbi—Ulbi Perevalochnaya	2488	1980	1715	1587	1400
7	Oba—Shemonaikha	3497	2917	2615	2462	2236
8	Shar—Kentarlau	168	129	109	99.1	85.1
9	Yertis—Semiyarka	5127	4711	4480	4364	4187

The Yertis River is characterized by the highest values of maximum water discharges, making it the primary source of regional flood hazard. The Buktyrma and Ulbi tributaries possess high flood potential and, under extreme conditions, can generate discharges exceeding 2000–3000 m^3/s. The Kurshim, Naryn, and Shar rivers are distinguished by significantly lower absolute water availability yet exhibit substantial variability, which creates a threat of local floods. The most flood-prone reaches of the basin are associated with the Yertis, Oba, and Buktyrma rivers.

3.3. Uncertainty Assessment of Design Characteristics

The results of the uncertainty assessment for the design extreme characteristics of the maximum discharge series are presented in Table 11. The results of the uncertainty assessment for the design extreme characteristics of the maximum water-level series are presented in Table 12.

Analysis of the results shows that the magnitude of uncertainty depends significantly on the hydrological characteristics of the watercourses and the structure of the time series. For maximum water discharges, it was found that the relative uncertainty is significant and varies in the range from 12 to 59%. The highest values are characteristic of small watercourses (Naryn, Kurshim, Shar), where the relative variability of extreme values is greatest. For large rivers, the uncertainty is lower, at approximately 12–24%, which is associated with greater stability of the hydrological regime.

Table 11. Uncertainty assessment of calculated maximum water discharge (bootstrap).

River—Hydrological Station	$Q_{1\%}$ (Calculated), m^3/s	Lower Limit, m^3/s	Upper Limit, m^3/s	Interval Width, Δ m^3/s	Relative Uncertainty, U%
Kara Yertis—Boran	2162	1895	2372	477	22.1
Kurshim—Voznesenka	1175	941	1414	473	40.3
Naryn—Ulken Naryn	121	89.1	160	70.9	58.6
Buktyrma—Lesnaya Pristan	2520	2114	2929	815	32.3
Yertis—Ust-Kamenogorsk	2183	1622	2529	907	41.5
Ulbi—Ulbi Perevalochnaya	3120	2708	3467	759	24.3
Oba—Shemonaikha	146	114	182	68.0	46.6
Shar—Kentarlau	2592	2392	2701	309	11.9
Yertis—Semiyarka	4209	3989	4571	582	13.8

Table 12. Uncertainty assessment of calculated maximum water levels (bootstrap).

River—Hydrological Station	$Q_{1\%}$ (Calculated), m^3/s	Lower Limit, m^3/s	Upper Limit, m^3/s	Interval Width, Δ m^3/s	Relative Uncertainty, U%
Kara Yertis—Boran	562	528	603	75.0	13.3
Kurshim—Voznesenka	388	361	411	50.0	12.9
Naryn—Ulken Naryn	275	246	303	57.0	20.7
Buktyrma—Lesnaya Pristan	719	657	781	124	17.2
Yertis—Abylaikit	508	465	540	75.1	14.8
Ulbi—Ulbi Perevalochnaya	427	398	457	58.6	13.8
Oba—Shemonaikha	508	476	539	63.6	12.4
Yertis—Semey	603	547	659	112	18.6
Yertis—Semiyarka	688	604	769	165	24.0
Yertis—Pavlodar	807	756	881	125	15.5
Yertis—Zhanabet (Bobrovsky)	551	537	571	33.8	6.20
Yertis—Yertis	763	739	788	48.9	6.40

It should be noted that the increase in uncertainty for rare quantiles is an expected result and is associated with the high sensitivity of the distribution tails to single extreme events, as well as with the uncertainty of the parameters of statistical models. Overall, the obtained values indicate acceptable stability of the calculated characteristics, while emphasizing the need for cautious interpretation of rare return period estimates, especially for small watercourses.

For maximum water levels, it was found that the uncertainty is generally lower, ranging from 6% to 24% for most stations, indicating a more stable nature of this parameter. The lowest uncertainty is observed at the Yertis—Zhanabet and Yertis—Priirtyshskoye stations, which is attributed to the relatively stable hydrological structure of the time series. The highest uncertainty values are observed at the Naryn—Ulken Naryn and Yertis—Semiyarka hydrological stations, which is due to high interannual variability and lower absolute values of the levels. Overall, the results demonstrate that, on average across the basin, the uncertainty is approximately 15%, indicating acceptable reliability of the estimates of extreme characteristics.

4. Discussion

In this study, the integration of statistical analysis of hydrological series with geoinformation modeling for mapping flood zones in the middle and lower reaches of the Yertis River has been implemented. It should be noted that the results obtained are probabilistic in nature and are based on statistical analysis of time series. The approach used does not account for the hydrodynamic processes involved in flood formation, such as channel deformations, the dynamics of flood wave propagation, and the spatial structure of inundation.

However, the results obtained should be considered as a basis for further hydrodynamic calculations and engineering assessments.

The results of modeling have shown that the highest concentration of risks is observed in the middle reaches (areas of the cities of Pavlodar, Semey, Oskemen), where water levels for the availability of 0.1% and 10% exceed the average long-term values by 1.5–2 times. confirming that the hydrological regime of the river is formed under the combined influence of climatic factors and morphometric characteristics of the channel and floodplain [59,60]. The presented approach has a number of limitations. In particular, it is based on stationary statistical analysis and does not account for the hydrodynamic processes involved in flood formation. The results obtained should be regarded as a preliminary assessment of potential risk, which can serve as a basis for more detailed studies using hydrodynamic models. It should be noted that the degree of uncertainty increases significantly for hydrological stations with high interannual variability and anthropogenic influence (flow regulation). This is particularly evident for the middle reaches of the Yertis River (Pavlodar, Semey), where the significant width of the confidence intervals reflects a complex hydrological regime caused by a combination of natural and regulatory factors.

The identified local flood zones, which do not coincide with traditional risk maps, are explained by the complex geometry of the floodplain microrelief and the influence of lateral inflow. This is consistent with the results of studies highlighting the importance of taking into account detailed topography and subpixel features of the terrain when modeling the spread of floods [61,62]. The presence of microrelief significantly affects local flooding scenarios, which is confirmed by similar findings for the river basins considered in the works [63,64]. In contrast to the earlier work on the Yertis River basin, which was limited to the analysis of data from individual hydrological stations or the use of low-spatial detail models, the proposed approach made it possible to switch to distributed risk analysis. This is in line with the global trend towards the use of integrated geographic information systems and statistical methods for spatially accurate assessment of hydrological hazards [52].

The observed differences in the quality of the approximations and in the distribution parameters reflect the physical characteristics of how peak discharges and water levels are formed in the Yertis River basin. The tributaries Kurshim, Naryn, and Buk-Tyrma are characterized by a more stable flood formation regime, which leads to a more compact distribution of extreme values and, consequently, to less uncertainty in the calculated characteristics. At the same time, for the lowland sections of the Yertis River, higher interannual variability of maximum values is observed, which is associated with the combined influence of climatic factors as well as the regulation of the flow. The influence of reservoirs leads to a transformation of the natural flow regime, the smoothing of flood peaks, and a change in the statistical structure of time series, which is reflected in a deterioration in the quality of the approximation for individual hydrological stations.

It should be noted that the observed characteristics of the distribution of extreme values may be associated with contemporary climate change. Rising air temperatures in the region, changes in the structure of atmospheric precipitation, and an increase in the frequency of extreme hydrometeorological events lead to increased variability in river flow. In particular, earlier snowmelt, changes in the intensity of spring processes, and an increase in the proportion of rain-fed runoff can lead to changes in the characteristics of spring floods and, consequently, to a transformation of the statistical distributions of extreme values. In this study, these processes are taken into account indirectly through the analysis of observed time series; however, their explicit modeling requires the use of non-stationary approaches and climate scenarios, which are beyond the scope of this work. The results obtained can serve as a basis for subsequent integration with hydrodynamic models and

the assessment of territorial vulnerability, which will allow a transition from a probabilistic assessment of extreme characteristics to a comprehensive flood risk assessment.

The integration of multi-year time series (1974–2025) and GIS modeling made it possible to achieve a higher accuracy of forecast compared to deterministic approaches, which is also noted in international practice [65].

The developed flood-zone maps for the cities of Pavlodar, Semey, and Oskemen provide a basis for transitioning from reactive response to preventive planning of damage reduction measures. The integration of modeling results with infrastructure data enhances the efficiency of evacuation planning, the design of protective structures, and the assessment of socioeconomic asset exposure. The use of a Digital Elevation Model (SRTM) with a resolution of 30 m allowed for achieving adequate accuracy at the regional level; however, it limits the detail when modeling urbanized territories. Similar limitations are noted in international studies, which emphasize the influence of digital elevation model resolution on the accuracy of risk assessment [66]. The lack of publicly available digital elevation models with a resolution of up to 1 m remains a key limitation for hydrological studies of large basins. A promising direction is the use of LiDAR data and UAV aerial photography to create high-resolution digital elevation models and improve modeling accuracy in urban zones [67]. Furthermore, the integration of static risk maps into early warning systems will allow for modeling flood wave dynamics in real-time, which aligns with modern trends in the development of adaptive risk management systems.

The proposed approach offers several advantages over traditional flood modeling methods. Unlike hydrodynamic models, it does not require the specification of complex boundary conditions, making it applicable in situations where data is limited. An additional advantage is the reproducibility of results, ensured by the use of formalized statistical criteria (the Kolmogorov–Smirnov test, the Akaike information criterion) and the transparency of the model selection procedure. At the same time, it should be emphasized that the proposed method does not replace hydrodynamic modeling, but rather serves as a preliminary assessment tool that allows for the identification of potentially hazardous areas and provides a basis for further detailed studies.

5. Conclusions

The results of the study showed that the hydrological regime of the Yertis River basin during the period 1974–2025 is characterized by high spatial and temporal variability and a trend toward an increase in the frequency of high and extreme spring floods. It has been established that the greatest intensity of hydrological extremes is characteristic of the middle reaches of the Yertis River and the basins of its major tributaries—the Buktyrma, Ulbi, and Oba—where the highest water levels and discharge rates are recorded, as well as a pronounced cyclical pattern of flood activity. In contrast, the basins of the Naryn and Kurshim rivers are characterized by a more stable regime with a smaller amplitude of fluctuations; however, even here, an increase in the recurrence of high floods has been observed since the 2000s.

Statistical analysis of long-term time series revealed the presence of cycles of increased water abundance, most clearly evident in the early 1990s, the mid-2010s, and the current period of the 2020s. Extreme floods occur infrequently (once every 25–50 years), but pose the greatest risks to the population, infrastructure, and floodplain areas. For a number of hydrological stations (Yertis—Pavlodar, Yertis—Priirtyshskoye, Yertis—Semiyarka, Buktyrma—Lesnaya Pristan), a trend has been identified toward an increase in the frequency of high spring floods and a widening of the range of interannual variability, indicating an intensification of climate instability.

The integration of statistical analysis of hydrological time series with geoinformation modeling enabled a spatially detailed assessment of flood zones and revealed that the highest flood risk is characteristic of the urban areas of Semey, Pavlodar, and Oskemen. It is shown that the formation of flood zones is determined by the complex interaction of climatic factors, the morphometric characteristics of the river channel and floodplain, glacial recharge, and anthropogenic regulation of flow. The results confirm that reservoirs, on the one hand, help smooth out peak water flows, and on the other hand, alter the structure of floods and the duration of high-water levels.

The study's findings suggest that the current transformation of the hydrological regime of the Yertis River basin reflects an increase in climate-driven variability of river flow and a higher probability of hazardous hydrological events. The developed models and flood-zone maps can serve as a scientific basis for improving flood forecasting systems, spatial planning, and the development of adaptation measures to reduce flood risk in a changing climate.

Supplementary Materials: The following supporting information can be downloaded at: https://www.mdpi.com/article/10.3390/environments13060303/s1, Table S1: Frequency and availability of maximum water levels.

Author Contributions: Conceptualization, L.M. and S.A.; methodology, L.M. and A.M.; software, A.M., T.I. and G.B.; validation, E.T., A.A., T.I. and A.Z.; formal analysis, L.M. and L.B.; investigation, L.B., B.I. and Z.B.; data curation, G.B., A.A., B.I. and O.A.; writing—original draft preparation, L.M. and M.L.; writing—review and editing, S.A., L.M., A.M., M.L. and A.A.; visualization, A.M., E.T. and A.Z.; supervision, L.M.; project administration, S.A.; funding acquisition, S.A., Z.B. and L.M. All authors have read and agreed to the published version of the manuscript.

Funding: This research was funded by the Science Committee of the Ministry of Science and Higher Education of the Republic of Kazakhstan, Grant No. BR28713279 "Scientific and Applied Foundations for Flood Risk Management in the Flat and Low-Hilly Territories of Kazakhstan under Modern Climate Change Conditions".

Data Availability Statement: The data presented in this study may be obtained on request from the corresponding author.

Conflicts of Interest: The authors declare no conflicts of interest.

References

1. Merz, B.; Hall, J.; Disse, M.; Schumann, A. Fluvial flood risk management in a changing world. *Nat. Hazards Earth Syst. Sci.* **2010**, *10*, 509–527. [CrossRef]
2. Ward, P.J.; Jongman, B.; Weiland, F.S.; Bouwman, A.; van Beek, R.; Bierkens, M.F.P.; Ligtvoet, W.; Winsemius, H.C. Assessing flood risk at the global scale: Model setup, results, and sensitivity. *Environ. Res. Lett.* **2013**, *8*, 044019. [CrossRef]
3. Plekhanov, P.A. Natural hydrological risks and their prevention in Kazakhstan. *Cent. Asian J. Water Res.* **2017**, *3*, 17–23.
4. United Nations Office for Disaster Risk Reduction. *Sendai Framework for Disaster Risk Reduction 2015–2030*; United Nations: Geneva, Switzerland, 2015. Available online: https://www.unisdr.org/files/43291_russiansendaiframeworkfordisasterri.pdf (accessed on 25 October 2025).
5. Plekhanov, P.A.; Popov, N.V.; Medeu, N.N.; Nikiforova, L.N. Moduli of maximum runoff in snow melt floods on rivers of the southeastern part of Esil River basin. *Int. J. Eng. Res. Technol.* **2020**, *13*, 1314–1318. Available online: https://www.ripublication.com/irph/ijert20/ijertv13n6_32.pdf (accessed on 27 April 2026). [CrossRef]
6. Akiyanova, F.; Ongdas, N.; Zinabdin, N.; Karakulov, Y.; Nazhbiyev, A.; Mussagaliyeva, Z.; Atalikhova, A. Operation of gate-controlled irrigation system using HEC-RAS 2D for spring flood hazard reduction. *Computation* **2023**, *11*, 27. [CrossRef]
7. Makhmudova, L.; Moldakhmetov, M.; Mussina, A.; Sambetbayev, D.; Zharylkassyn, A. Flood hazard assessment in the Yesil River basin. *AQUA Water Infrastruct. Ecosyst. Soc.* **2023**, *72*, 1499–1511. [CrossRef]
8. Sanders, B.F.; Schubert, J.E.; Kahl, D.T.; Mach, K.J.; Brady, D.; AghaKouchak, A.; Forman, F.; Matthew, R.A.; Ulibarri, N.; Davis, S.J. Large and inequitable flood risks in Los Angeles, California. *Nat. Sustain.* **2023**, *6*, 47–57. [CrossRef]

9. Liu, W.; Feng, Q.; Engel, B.A.; Yu, T.; Zhang, X.; Qian, Y. A probabilistic assessment of urban flood risk and impacts of future climate change. *J. Hydrol.* **2023**, *618*, 129267. [CrossRef]
10. Heinrich, D.F.; Penning-Rowsell, E.C. Flood risk management under uncertainty in transboundary basins: A delicate balancing act. *Int. J. River Basin Manag.* **2022**, *20*, 215–224. [CrossRef]
11. Aven, T. Risk assessment and risk management: Review of recent advances on their foundation. *Eur. J. Oper. Res.* **2016**, *253*, 1–13. [CrossRef]
12. Kron, W. Flood Risk = Hazard • Values • Vulnerability. *Water Int.* **2005**, *30*, 58–68. [CrossRef]
13. Mussina, A.; Abdullayeva, A.; Zhanabayeva, Z.; Rakhimova, M.; Akhmetova, M.; Kozhakhmetova, U.; Liu, T.; Taukebayev, O. GIS and RS data-based morphometric analysis of the Talas River watershed characteristics. *Hydrol. Res.* **2025**, *56*, 572–592. [CrossRef]
14. Intergovernmental Panel on Climate Change. *Global Warming of 1.5 °C: An IPCC Special Report on the Impacts of Global Warming of 1.5 °C above Pre-Industrial Levels and Related Global Greenhouse Gas Emission Pathways*; IPCC: Geneva, Switzerland, 2018. Available online: https://www.ipcc.ch/sr15/ (accessed on 10 December 2025).
15. Intergovernmental Panel on Climate Change. *Climate Change 2022: Impacts, Adaptation and Vulnerability. Contribution of Working Group II to the Sixth Assessment Report of the IPCC*; IPCC: Geneva, Switzerland, 2022. Available online: https://www.ipcc.ch/report/ar6/wg2/ (accessed on 10 December 2025).
16. Central Asia Regional Economic Cooperation Program. *Country Risk Profile: Kazakhstan. TA-9878 REG: Strengthening Disaster Risk Transfer Mechanisms in the CAREC Region*; CAREC Program: Manila, Philippines, 2022. Available online: https://www.carecprogram.org/uploads/Country_Risk_Profiles_Kazakhstan_RU.pdf (accessed on 5 December 2025).
17. Bates, P.D.; De Roo, A.P.J. A simple raster-based model for flood inundation simulation. *J. Hydrol.* **2000**, *236*, 54–77. [CrossRef]
18. Horritt, M.S.; Bates, P.D. Evaluation of 1D and 2D numerical models for predicting river flood inundation. *J. Hydrol.* **2002**, *268*, 87–99. [CrossRef]
19. Haghizadeh, A.; Siahkamari, S.; Haghiabi, A.H.; Rahmati, O. Forecasting Flood-Prone Areas Using Shannon's Entropy Model. *J. Earth Syst. Sci.* **2017**, *126*, 39. [CrossRef]
20. Pradhan, B. Flood Susceptible Mapping and Risk Area Delineation Using Logistic Regression, GIS and Remote Sensing. *J. Spat. Hydrol.* **2009**, *9*, 1–18.
21. Aksoy, H.; Kirca, V.S.O.; Burgan, H.I.; Kellecioglu, D. Hydrological and Hydraulic Models for Determination of Flood-Prone and Flood Inundation Areas. *Proc. Int. Assoc. Hydrol. Sci.* **2016**, *373*, 137–141. [CrossRef]
22. Ghosh, A.; Chatterjee, U.; Pal, S.C.; Towfiqul Islam, A.R.M.; Alam, E.; Islam, M.K. Flood Hazard Mapping Using GIS-Based Statistical Model in Vulnerable Riparian Regions of Sub-Tropical Environment. *Geocarto Int.* **2023**, *38*, 2285355. [CrossRef]
23. Farid, M.; Dewi, N.T.; Adityawan, M.B.; Nugroho, E.O.; Alhamid, A.K.; Wahid, A.N.; Sihombing, Y.I. Probabilistic urban flood risk assessment of multi-sectoral economic losses due to levee overtopping. *Results Eng.* **2025**, *27*, 106260. [CrossRef]
24. Gün, R.; Yılmaz, M. A New Framework for Comprehensive Flood Risk Assessment under Non-Stationary Conditions Using GIS-Based MCDM Modeling. *Atmosphere* **2026**, *17*, 62. [CrossRef]
25. Makhmudova, L.; Alimkulov, S.; Mussina, A.; Vangelis, H.; Talipova, E.; Alzhanov, O.; Moldakhanova, N.; Imamova, B.; Iskakova, G.; Birimbayeva, L.; et al. Compound Drivers of Extreme Spring Floods in a Changing Climate: The Esil River Case, Kazakhstan. *Earth Syst. Environ.* 2026; *in press*. [CrossRef]
26. El Haou, M.; Ourribane, M.; Ismaili, M.; Abdelrahman, K.; Fnais, M.S.; Krimissa, S.; El Oudi, H.; Hajji, S.; El Bouzkraoui, M.; Tarchi, F.; et al. Advanced GIS-based modeling for flood hazards mapping in urban semi-arid regions: Insights from Beni Mellal, Morocco. *Front. Environ. Sci.* **2025**, *13*, 1585926. [CrossRef]
27. Li, Q.; Ni, T.; Li, L.; Wen, H.; Xu, J. A probabilistic GIS-based framework for urban flood risk assessment in Chengdu metro network. *Sci. Rep.* **2025**, *15*, 43526. [CrossRef] [PubMed]
28. Zhomartkan, N.; Pavlenko, A.; Baiburin, Y.; Alhuyi-Nazari, M. Modeling and Web-Based Visualization of Flood Zones: A Case Study of the Buktyrma River Section. *Sci. J. Astana IT Univ.* **2025**, *23*, 215–230. [CrossRef]
29. Shugulova, D.K.; Mazhitova, G.Z.; Dzhanaleeva, K.M. Determination of Flooded Areas Using GIS Modeling of Hydrological Processes. *Bull. L.N. Gumilyov Eurasian Natl. Univ. Chem. Geogr. Ecol. Ser.* **2022**, *2*, 72–79. (In Russian) [CrossRef]
30. Apshikur, B.; Kurmangaliyev, T.B.; Goltsev, A.G.; Alimkulov, M.M.; Kapasov, A.K. The Method of Multi-Criteria Analysis for Determining the Flood-Hazardous Area and the Development of Protective Structures. *Int. Arch. Photogramm. Remote Sens. Spat. Inf. Sci.* **2023**, *XLVIII-5/W2-2023*, 9–17. [CrossRef]
31. Shugulova, D.; Mazhitova, G.; Makhanova, N.; Pashkov, S.; Asylbekov, K.; Berdenov, Z. Geoinformation Modeling of the Esil River Flood Zone Based on Remote Sensing Data. *J. Geogr. Environ. Manag.* **2023**, *69*, 60–69. [CrossRef]
32. Kazhydromet RSE. Available online: https://www.kazhydromet.kz/en/ (accessed on 15 January 2026).
33. Nosach, V.P.; Sikan, A.V. Study of the probabilistic structure of maximum runoff series of Karelia rivers. *Gidrol. Okeanol.* **2023**, 81–88. (In Russian)

34. Sikan, A.V.; Shcheglov, D.A. Assessment of errors in sample parameters of hydrological series distributions. In Proceedings of the Fourth Vinogradov Readings: Hydrology from Knowledge to Worldview, St. Petersburg, Russia, 2–4 March 2020; pp. 530–535. (In Russian)
35. Sikan, A.V.; Vinokurov, I.O.; Teslenko, D.D. Application of the L-moment method for estimating parameters of maximum spring flood discharge distribution in rivers of Northwest Russia. *Uchenye Zap. Ross. Gos. Gidrometeorol. Univ.* **2015**, *38*, 21–27. (In Russian)
36. Sikan, A.V. Optimization of distribution parameters for constructing exceedance probability curves of extreme water discharges. *Uchenye Zap. Ross. Gos. Gidrometeorol. Univ.* **2012**, *24*, 26–32. (In Russian)
37. Akaike, H. A new look at the statistical model identification. *IEEE Trans. Autom. Control* **1974**, *19*, 716–723. [CrossRef]
38. Laio, F.; Di Baldassarre, G.; Montanari, A. Model selection techniques for the frequency analysis of hydrological extremes. *Water Resour. Res.* **2009**, *45*, W07416. [CrossRef]
39. Rahman, A.; Haddad, K.; Zaman, M.; Ahsan, A. Flood frequency analysis in Australia: Empirical investigation of probability distributions and parameter estimation techniques. *Nat. Hazards* **2013**, *69*, 1803–1813. [CrossRef]
40. Stephens, M.A. EDF statistics for goodness of fit and some comparisons. *J. Am. Stat. Assoc.* **1974**, *69*, 730–737. [CrossRef]
41. Hosking, J.R.M. L-moments: Analysis and estimation of distributions using linear combinations of order statistics. *J. R. Stat. Soc. Ser. B* **1990**, *52*, 105–124. [CrossRef]
42. Katz, R.W.; Parlange, M.B.; Naveau, P. Statistics of extremes in hydrology. *Adv. Water Resour.* **2002**, *25*, 1287–1304. [CrossRef]
43. Teegavarapu, R.S.V.; Chandramouli, V. Improved weighting methods, deterministic and stochastic data-driven models for estimation of missing precipitation records. *J. Hydrol.* **2005**, *312*, 191–206. [CrossRef]
44. Cunnane, C. Statistical distributions for flood frequency analysis. In *Operational Hydrology Report No. 33*; World Meteorological Organization (WMO): Geneva, Switzerland, 1989.
45. Shelutko, V.A. *Methods for Processing and Analysis of Hydrological Information*; St. Petersburg State University Publishing House: Saint Petersburg, Russia, 2007; 192p. (In Russian)
46. Seredovskikh, B.A. Hydrological hazards in the Konda River basin. *Vestn. Surgutskogo Gos. Pedagog. Univ.* **2022**, *6*, 164–176. (In Russian) [CrossRef]
47. Seredovskikh, B.A.; Nevolin, N.A. Research and mapping of channel deformations of the Konda River. In *Culture, Science, Education: Problems and Prospects. Proceedings of the VII All-Russian Scientific and Practical Conference with International Participation*; Pogonyshev, D.A., Ed.; Nizhnevartovsk State University Publishing House: Nizhnevartovsk, Russia, 2019; pp. 84–88. (In Russian)
48. Sanders, B.F. Evaluation of on-line DEMs for flood inundation modeling. *Adv. Water Resour.* **2007**, *30*, 1831–1843. [CrossRef]
49. Cook, A.; Merwade, V. Effect of topographic data, geometric configuration and modeling approach on flood inundation mapping. *J. Hydrol.* **2009**, *377*, 131–142. [CrossRef]
50. Yamazaki, D.; Ikeshima, D.; Tawatari, R.; Yamaguchi, T.; O'Loughlin, F.; Neal, J.C.; Sampson, C.C.; Kanae, S.; Bates, P.D. A high-accuracy map of global terrain elevations. *Geophys. Res. Lett.* **2017**, *44*, 5844–5853. [CrossRef]
51. Teng, J.; Jakeman, A.J.; Vaze, J.; Croke, B.F.W.; Dutta, D.; Kim, S. Flood inundation modelling: A review of methods, recent advances and uncertainty analysis. *Environ. Model. Softw.* **2017**, *90*, 201–216. [CrossRef]
52. Merwade, V.; Cook, A.; Coonrod, J. GIS techniques for creating river terrain models for hydrodynamic modeling and flood inundation mapping. *Environ. Model. Softw.* **2008**, *23*, 1300–1311. [CrossRef]
53. Bates, P.D.; Horritt, M.S.; Fewtrell, T.J. A simple inertial formulation of the shallow water equations for efficient two-dimensional flood inundation modelling. *J. Hydrol.* **2010**, *387*, 33–45. [CrossRef]
54. Di Baldassarre, G.; Schumann, G.; Bates, P.D.; Freer, J.E.; Beven, K.J. Flood-plain mapping: A critical discussion of deterministic and probabilistic approaches. *Hydrol. Sci. J.* **2010**, *55*, 364–376. [CrossRef]
55. Kurakina, N.I.; Kovchik, V.S. Geoinformation system for modelling hydrological flooding processes. *Izv. SPbGETU "LETI"* **2020**, *5*, 66–73. (In Russian)
56. Efron, B.; Tibshirani, R.J. *An Introduction to the Bootstrap*; Chapman & Hall/CRC: Boca Raton, FL, USA, 1993.
57. Ma, B.; Guo, J.; Chen, P.; Zhang, L.; Wang, H.; Zhou, Y.; Sun, B. Comprehensive risk assessment of urban floods based on flood simulation and socio-economic vulnerability. *Front. Earth Sci.* **2025**, *13*, 1645693. [CrossRef]
58. Farooq, O.; Khalil, M.N.; Mahmood, R.S.; Jan, A. Flood risk assessment and management using hydrological modeling and GIS technique. *Policy Res. J.* **2026**, *4*, 381–391. [CrossRef]
59. Tehrany, M.S.; Pradhan, B.; Jebur, M.N. Flood susceptibility mapping using a novel ensemble weights-of-evidence and support vector machine models in GIS. *J. Hydrol.* **2014**, *512*, 332–343. [CrossRef]
60. Khosravi, K.; Shahabi, H.; Pham, B.T.; Adamowski, J.; Shirzadi, A.; Pradhan, B.; Dou, J.; Ly, H.-B.; Gróf, G.; Ho, H.L.; et al. A comparative assessment of flood susceptibility modeling using multi-criteria decision-making analysis and machine learning methods. *J. Hydrol.* **2019**, *573*, 311–323. [CrossRef]
61. Kourgialas, N.N.; Karatzas, G.P. Flood management and a GIS modelling method to assess flood-hazard areas—A case study. *Hydrol. Sci. J.* **2011**, *56*, 212–225. [CrossRef]

62. Wing, O.E.J.; Bates, P.D.; Smith, A.M.; Sampson, C.C.; Johnson, K.A.; Fargione, J.; Morefield, P. Estimates of present and future flood risk in the conterminous United States. *Environ. Res. Lett.* **2018**, *13*, 034023. [CrossRef]
63. Sampson, C.C.; Smith, A.M.; Bates, P.D.; Neal, J.C.; Alfieri, L.; Freer, J.E. A high-resolution global flood hazard model. *Water Resour. Res.* **2015**, *51*, 7358–7381. [CrossRef]
64. Dottori, F.; Salamon, P.; Bianchi, A.; Alfieri, L.; Hirpa, F.; Feyen, L. Development and evaluation of a framework for global flood hazard mapping. *Adv. Water Resour.* **2016**, *94*, 87–102. [CrossRef]
65. De Moel, H.; Jongman, B.; Kreibich, H.; Merz, B.; Penning-Rowsell, E.; Ward, P.J. Flood risk assessments at different spatial scales. *Mitig. Adapt. Strateg. Glob. Change* **2015**, *20*, 865–890. [CrossRef] [PubMed]
66. Saksena, S.; Merwade, V. Incorporating the effect of DEM resolution and accuracy for improved flood inundation mapping. *J. Hydrol.* **2015**, *530*, 180–194. [CrossRef]
67. Mussina, A.; Tursyngali, M.; Duskayev, K.; Rodrigo-Ilarri, J.; Rodrigo-Clavero, M.-E.; Abdullayeva, A. Forecasting channel morphodynamics in the Ulken Almaty River (Ile Alatau, Kazakhstan). *Water* **2025**, *17*, 2029. [CrossRef]

Disclaimer/Publisher's Note: The statements, opinions and data contained in all publications are solely those of the individual author(s) and contributor(s) and not of MDPI and/or the editor(s). MDPI and/or the editor(s) disclaim responsibility for any injury to people or property resulting from any ideas, methods, instructions or products referred to in the content.